MASS. INST. OF TECHNOLOGY
MAY 1 1964
LIBRARIES

STRAPPED-DOWN GYRO DRIFT CORRECTION FROM POSITION FIXES

by

Guy M. Fujimoto
S.B.E.E., Massachusetts Institute of Technology
(1960)

SUBMITTED IN PARTIAL FULFILLMENT OF THE
REQUIREMENTS FOR THE DEGREE OF
MASTER OF SCIENCE
at the
MASSACHUSETTS INSTITUTE OF TECHNOLOGY

August, 1963

Signature of Author _____
Department of Electrical Engineering, August 19, 1963

Certified by _____
Thesis Supervisor

_____
Thesis Supervisor

Accepted by _____
Chairman, Departmental Committees on Graduate Students

STRAPPED-DOWN GYRO DRIFT CORRECTION FROM POSITION FIXES

by

Guy Michael Fujimoto

Submitted to the Department of Electrical Engineering on August 19, 1963 in partial fulfillment of the requirement for the degree of Master of Science.

ABSTRACT

Errors in an inertial navigation system produced by gyro drift tend to accumulate with time. The determination and subsequent removal of gyro drift is therefore mandatory if the system is to remain within operational specifications over extended periods of time. The object of this thesis is to devise a means of determining gyro drift in a "modified-strapped-down" system using intermittently-obtained position and/or heading information. In the strapped-down configuration, relationships between system output errors and the drift of each gyro depend on the orientation of the vehicle relative to the navigation coordinate system. Thus, there is an unusual requirement that the method of gyro drift determination account for arbitrary motion of the vehicle.

The only additional equipment required by the method of this thesis is a special-purpose computer which will perform real-time multiplication and integration operations. In addition to determining gyro drift compensation, this scheme allows for the correction of system output errors.

As a realistic example, application of this reset method has been made to a strapped-down system for a submarine. An investigation into the possibility of reducing the required number of computations has also been made and includes several simulations of reset operations on a general-purpose high-speed digital computer.

Thesis Supervisor: Prof. H. Philip Whitaker
Title: Associate Professor of Aeronautics and Astronautics

Thesis Supervisor: John Hovorka, Sc.D.
Title: Lecturer in Aeronautics and Astronautics

ACKNOWLEDGEMENTS

The author wishes to express his appreciation to the personnel of the Instrumentation Laboratory who have assisted in this study. Particular thanks are due the following: to Dr. Joseph E. DeLisle and his group, in whose area this thesis was done; to Charles Broxmeyer and Aldo De Simone, who suggested the thesis topic and provided valuable technical assistance; and to Miss Nina L. Johnson for her patience and considerable skill in typing the manuscript. Special thanks are due to Professor H. P. Witaker and Dr. John Hovorka, the thesis supervisors, for their continued interest, guidance and helpful criticisms on the content of this thesis.

This thesis was prepared under the auspices of DSR Project 53-178, sponsored by the Director, Special Projects Office (SP-24), Department of Navy, under USN Contract NObs 78456 (FBM), dated 22 March 1960.

TABLE OF CONTENTS

		Page
Chapter 1	INTRODUCTION	7
Chapter 2	BACKGROUND OF THE RESET PROBLEM	10
2.1	Crude Form of Reset	10
2.2	Inertial Navigation System Reset	10
2.3	The Drift Circle	13
2.4	Reset Using the Drift Circle	16
Chapter 3	THE MODIFIED-STRAPPED-DOWN SYSTEM	20
3.1	Gimbaled Systems	20
3.2	The Strapped-Down System	20
3.3	Advantages and Disadvantages of the Strapped-Down System	21
3.3.1	The Torquing Accuracy Problem	21
3.3.2	The Output-Axis Torque Problem	22
3.3.3	The Cross-Coupling Torque Problem	22
3.4	The Modified-Strapped-Down Inertial Navigation System	22
3.4.1	The Inertial Reference Unit	23
3.4.2	The Navigation System	26
Chapter 4	RESETTING THE STRAPPED-DOWN SYSTEM	
4.1	The Problem	31
4.2	The Proposed Solution	32
Chapter 5	THE SUBMARINE APPLICATION	39
5.1	The Submarine Application as an Example	39
5.2	Derivation of the Error Matrix	39
5.3	The Error Transfer Functions	45

TABLE OF CONTENTS (cont)

5.4 Drift Forcing Functions 48

5.4.1 Constant Drift 49

5.4.2 Mass Unbalance Drift 50

5.5 Determination of the Drift Constants 54

5.6 The Reset Operation 56

5.7 Discussion. 57

Chapter 6 SIMPLIFICATIONS AND SIMULATIONS 60

6.1 Simplifications 60

6.2 Submarine Motion 61

6.2.1 The Model 61

6.3 The Weighting Function 69

6.4 Simulations 70

6.5 Discussion of the Simulation Results 78

Chapter 7 SUMMARY, CONCLUSIONS, AND RECOMMENDATIONS .

7.1 Summary 79

7.2 Conclusions 80

7.3 Recommendations 80

Appendix A Derivation of the Error Matrix for a Gimbaled System 81

Appendix B Strapped-Down System Error Equations 87

Appendix C Derivation of the Motion Model's Spectra 92

Appendix D Block Diagram of the Simulation Program 96

Bibliography. 98

LIST OF ILLUSTRATIONS

		Page
Figure 2.1	Drift Circle	17
Figure 3.1	Schematic Diagram of an Inertial Reference Unit	24
Figure 3.2	Schematic Diagram of the Complete Inertial Reference Unit	27
Figure 3.3	Functional Diagram of the Inertial Navigation System	30
Figure 5.1	Flow Diagram of the Error Equations	46
Figure 5.2	Definition of θ_x	52
Figure 6.1	Energy Spectrum of Roll Amplitude	62
Figure 6.2	Roll Motion Model ($M = 6.735°$, $\sigma = 4.76°$)	64
Figure 6.3	Roll Motion Model ($M = 15°$, $\sigma = 10.5°$)	64
Figure 6.4	Autocorrelation Function of Model.	66
Figure 6.5	Periodic Component of Autocorrelation Function	66
Figure 6.6	Random Component of Autocorrelation Function	66
Figure 6.7	Power Spectrum of Periodic Component	67
Figure 6.8	Power Density Spectrum of Random Component	67
Figure 6.9	System Errors Without Resets	72
Figure 6.10	Latitude Error With Resets	74
Figure 6.11	Longtitude Error With Resets.	75
Figure 6.12	Azimuth Error With Resets.	75

TABLES

Table 6.1	Simplified Reset Errors For Latitude and Longtitude Fixes	76
Table 6.2	Simplified Reset Errors For Latitude, Longtitude and Azimuth Fixes	77

CHAPTER 1

INTRODUCTION

In missions requiring high performance over extended periods of time, as in the case of a missile launching submarine, the accuracy of the inertial navigation system is maintained by periodically resetting the system. In general terms, the reset operation consists of changing various system parameters and inputs so as to eliminate or reduce system errors which tend to grow with time.

Considerable attention [redacted] has been focused on the reset problem for the conventional, gimbaled systems now in use aboard Polaris submarines. Little, if any, research has been done on resetting a gimballess, or strapped-down, inertial navigation system however, mainly because the need for such work did not exist. A stringent gyro torquing accuracy requirement, when using existing inertial reference units in the conventional strapped-down configuration, has precluded the use of such a system in long term missions requiring high accuracy. The requirement arises because gyros in a strapped-down system are subjected to much larger angular rates than are the "stabilized" gyros of a gimbaled system. In reference (4) it has been estimated that the required accuracy for torquing single-degree-of-freedom gyros in a navigation quality system is about seven parts in a hundred million, which is beyond the capability of the present state of the art of gyro torquing.

Another important problem associated with strapped-down systems is the computational one. In addition to solving the usual navigation equations, the system computer must also compute an orthogonal transformation matrix, which involves a set of nine first-order differential equations. Because the transformation matrix has a dominant role in overall system performance,

special attention must be paid to its mechanization. Several studies [4] [5] [redacted][7] have been made on the subject, and the results indicate that the problem does not appear to be an insurmountable one. In this thesis, the computational problem will be ignored, and all reset computations will be assumed to be made with no error.

A modified strapped-down system has recently been proposed by Charles Broxmeyer and Aldo De Simone, while both were with the MIT Instrumentation Laboratory, in which gyro torquing is not a prohibitive factor. Rather than having the gyro cases rigidly mounted directly to the vehicle as is done in the conventional strapped-down system, the proposed system consists of three separate single axis stable platforms in which only the input axes are fixed relative to the vehicle. Whereas in the conventional configuration, vehicle angular rotations are measured in the gyro torquing servo loops, angular motion in the modified system is monitored by accurate incremental encoders. The feasibility of this system depends on how well the reset problem can be solved.

Because the primary source of errors in inertial navigation systems is gyro drift, the heart of the reset operation consists of determining the proper compensation that must be applied to the gyros in order to remove the drift. Several techniques are presently used in resetting gimbaled systems, in which gyro drift information is obtained by examining system errors which exist after an interval of operating time. The errors are determined periodically by comparing system output data with data which is accurately measured external to the inertial system. Because motion of the gimbal mounted gyros is well behaved, relatively simple relationships exist between the drift of specific gyros and certain system errors. These relationships therefore allow for the determination of appropriate gyro compensation.

The reset problem for a strapped-down system is much more complex. Simple relationships between the system errors and the drift of specific gyros no longer exist because of the arbitrary motion and orientation of the gyros relative to the indicated coordinate frame in which the system equations are solved. The effects of the drifts of all three gyros now become coupled in the generation of system errors in a manner dependent on the arbitrary time history of the vehicle's motion.

The object of this thesis is to develop a method of resetting a strapped-down inertial navigation system. Of primary concern is the determination of gyro drift based on fix information.

A background of the reset problem is contained in Chapter 2. Because the reset problem has been, up to the present time, peculiar to submarine navigation systems, a discussion of the basic reset theory for this application is given.

Chapter 3 describes the modified strapped-down system with which this thesis is concerned.

In Chapter 4, a method for resetting the strapped-down system is developed.

Because the nature of this thesis is somewhat subjective, a submarine application of the proposed reset method is presented in Chapter 5.

Chapter 6 contains a discussion of digital computer simulations which were made for the submarine example.

The concluding remarks are presented in Chapter 7.

CHAPTER 2

BACKGROUND OF THE RESET PROBLEM

The term reset, as applied to inertial equipment, can be defined, in general terms, as the operation of making necessary corrections and adjustments to the system which 1) reduce the system output errors and 2) restrain the growth of these errors thereafter.

2.1 Crude Forms of Reset

The reset operation is not peculiar to complex inertial navigation systems. Relatively simple navigational aids such as the directional gyro or the barometric altimeter require that a reset procedure be employed in order to maintain the accuracy, and hence, the effectiveness of the device. The directional gyro must be periodically reset with external information. In most cases, this involves a correction using a magnetic compass reading at intervals of about fifteen minutes. The external information used to reset a barometric altimeter comes from ground station broadcasts of local barometric pressure. Both of these examples of resetting are very simple and only fulfill the condition of correcting output errors. No attempt is made to reduce the growth of errors thereafter.

2.2 Inertial Navigation System Reset

Output errors of an inertial navigation system may be caused by many factors. These include, initial misalignment of the reference coordinate system, gyro drift, non-linearities in accelerometers and torquers, and base motion disturbances by imperfect gimbal servos, to name a few. These all, independently or in combination, produce navigational errors. With the exception of the gyro drift errors, all errors are independent of

time and can be internally compensated for. However, gyro drift errors vary with time and tend to build up over long periods of time.

The reset problem in inertial navigation systems has been previously investigated in connection with the Ship's Inertial Navigation System (SINS) developed by the MIT Instrumentation Laboratory. Errors in such a system, which essentially operates on the surface of the earth, can be described by a set of differential equations containing oscillatory modes. The periods of these oscillations are associated with the 84 minute Schuler period and the 24 hour period of the sidereal day. It is this oscillatory behavior which permits errors in an unaided system to build up with time, irregardless of the quality of the basic inertial components. Thus additional information is needed in order to keep system output errors within operational specifications. The two forms of additional information most widely considered are ship's velocity, and position and heading fixes. The ship's velocity is obtained by measuring the speed of the ship through the water with a pitometer-log or a similar device. Position and heading information, when available, may be obtained in a variety of ways, among these are Loran systems, celestial trackers or even the Transit Satellite system.

If the difference between the inertial system's velocity output and the measured velocity is used as a correcting signal, errors in various parts of the system will be reduced. This operation has the effect of damping the oscillations in the system. However, errors in ship's speed caused by the speed log device or by ocean currents lead to large heading, or azimuth, errors if the 24 hour loop is damped in this manner. Therefore, another procedure must be used to damp the 24 hour oscillation without inducing large azimuth errors. This procedure has evolved into what is known as the reset operation.

Stated in general terms, the reset procedure 1) makes corrections to the system output errors which exist at the time the reset is made, and 2) applies proper gyro compensation such that the tendency for the growth of output errors is reduced. Although various methods of reset procedure exist, they are all characterized by the utilization of position and/or heading information obtained from a source external to the inertial system.

By comparing these "fix" measurements, which are made periodically, with the system's outputs, output errors are determined. Knowledge of the relationship between the errors and gyro drifts then allows for the determination of the drift present in the system. Therefore application of the required gyro compensation completes the reset operation. Although of a peculiar nature, resetting is a form of damping.

Early inertial navigation systems at sea used reset methods requiring what was effectively a continuous measurement of the ship's position. Although not very sophisticated, it allowed the system to operate under existing operational specifications.

The advent of the Polaris weapon system generated much activity in the reset problem area. Operating conditions and performance specifications became more demanding because of the use of the submarine as a missile launching platform, and the concomitant need to minimize vehicle exposure.

A substantial amount of research has been done on resetting the SINS system, which is the primary navigator for Polaris launching submarines. The MIT Instrumentation Laboratory[redacted], Sperry Gyroscope Company[redacted], and Dynamics Research Corporation[redacted] have been major contributors to this problem area.

The reset procedures most widely used in operational navigation systems at sea are based on the constant, or slowly varying, gyro drift model.

Because of the discrete nature of fixes, the navigation system has also been studied as a multiple-input, multiple-output sampled data system. [redacted] When random drift errors are assumed, the error analysis lends itself to the application of statistical optimization techniques.

Although many forms of resetting SINS exist, which assume the slowly varying "constant" drift model, they are all variations based on what is called the drift circle. Because of its simple nature, it offers much insight into the general reset problem.

2.3 The drift circle

The navigation system output errors, as derived in Appendix A, can be described by the set of linear differential equations shown in matrix form as equation (2-1).

If the geographic coordinate system is defined as an orthogonal system having the x-axis pointing north, the y-axis pointing east, and the z-axis down and normal to the reference ellipsoid, the notation of equation (2-1) is,

α = x component of the vector error angle between the actual and indicated geographic coordinate systems (x vertical error)

β = y component of the vector error angle between the actual and indicated coordinate systems (y vertical error)

γ = z component of the vector error angle between the actual and indicated coordinate systems (heading, or azimuth error)

λ = geographic latitude

λ_c = computed geographic latitude

$\delta\lambda = \lambda - \lambda_c$ = latitude error

U_x, U_y, U_z = gyro drift rates referred to the indicated coordinate system

Ω = earth rate

$\delta\omega_e$ = longitude rate error $\times$ cos λ

$\delta\omega_n$ = geographic latitude rate error

$$\begin{bmatrix} \dot{\delta\omega}_n \\ \dot{\delta\omega}_e \\ \dot{\delta\lambda} \\ \dot{\alpha} \\ \dot{\beta} \\ \dot{\gamma} \end{bmatrix} = \begin{bmatrix} 0 & -2\Omega\sin\lambda & 0 & 0 & g/R & 0 \\ 2\Omega\sin\lambda & 0 & 0 & -g/R & 0 & 0 \\ 1 & 0 & 0 & 0 & 0 & 0 \\ 0 & 1 & -\Omega\sin\lambda & 0 & -\Omega\sin\lambda & 0 \\ -1 & 0 & 0 & \Omega\sin\lambda & 0 & \Omega\cos\lambda \\ 0 & -\tan\lambda & -\Omega\cos\lambda & 0 & -\Omega\cos\lambda & 0 \end{bmatrix} \begin{bmatrix} \delta\omega_n \\ \delta\omega_e \\ \delta\lambda \\ \alpha \\ \beta \\ \gamma \end{bmatrix} + \begin{bmatrix} 0 \\ 0 \\ 0 \\ u_x \\ u_y \\ u_z \end{bmatrix} \qquad (2\text{-}1)$$

The characteristic equation of the error matrix expressed in Laplace notation is

$$\left[s^2+\Omega^2\right]\left[s^4+(4\Omega^2\sin^2\lambda+2g/R)s^2+(g/R)^2\right]=0 \qquad (2\text{-}2)$$

Thus, the system has oscillatory modes comprising three natural frequencies. Two of these frequencies are associated with the Schuler frequency and have periods near 84 minutes. The 84 minute oscillations are primarily involved with the vertical errors, α and β. As mentioned earlier, these errors can be damped to reasonably small values with the use of externally obtained velocity information. The third frequency has a period of 24 hours and is essentially a coupled oscillation between the azimuth error and the latitude error. It is this oscillation that the reset operation is intended to damp.

By multiplying the fourth equation of the matrix by sin λ and the sixth equation by cos λ and adding the two,

$$\begin{aligned}\dot{\alpha}\sin\lambda+\dot{\gamma}\cos\lambda &= \delta\omega_e\sin\lambda-\delta\lambda\,\Omega\sin^2\lambda-\beta\Omega\sin^2\lambda\\ &\quad+u_x\sin\lambda-\delta\omega_e\tan\lambda\cos\lambda\\ &\quad-\delta\lambda\,\Omega\cos^2\lambda-\beta\Omega\cos^2\lambda+u_z\cos\lambda\\ &= -\Omega(\delta\lambda+\beta)+u_x\sin\lambda+u_z\cos\lambda \qquad (2\text{-}3)\end{aligned}$$

Adding the third and fifth equations of the matrix,

$$\dot{\delta\lambda}+\dot{\beta}=\delta\omega_n-\delta\omega_n+\alpha\Omega\sin\lambda+\gamma\Omega\cos\lambda+u_y \qquad (2\text{-}4)$$

If the 84 minute oscillation is damped, terms in α and β can be neglected relative to terms in γ and $\delta\lambda$, and

$$\dot{\gamma}\cos\lambda=-\Omega\delta\lambda+u_x\sin\lambda+u_z\cos\lambda \qquad (2\text{-}5)$$

$$\dot{\delta\lambda}=\Omega\gamma\cos\lambda+u_y \qquad (2\text{-}6)$$

If $U_e = U_x \sin\lambda + U_z \cos\lambda$, ($U_e$ would be the equatorial gyro drift in the normal four or five-gimbal mode) (2-5) and (2-6) become,

$$\dot{\gamma}\cos\lambda = -\Omega\,\delta\lambda + \mathcal{U}_e \tag{2-7}$$

$$\delta\dot{\lambda} = \Omega\,\gamma\cos\lambda + \mathcal{U}_y \tag{2-8}$$

The characteristic equation of this set is,

$$\left[s^2 + \Omega^2\right] = 0$$

which clearly displays the 24 hour oscillation.

The quotient of equation (2-7) and (2-8) can be written using differentials as,

$$\frac{d\,\gamma\cos\lambda}{d\,\delta\lambda} = \frac{-\delta\lambda + \mathcal{U}_e/\Omega}{\gamma\cos\lambda + \mathcal{U}_y/\Omega} \tag{2-9}$$

Integrating (2-9),

$$\left(\gamma\cos\lambda + \mathcal{U}_y/\Omega\right)^2 + \left(\delta\lambda - \mathcal{U}_e/\Omega\right)^2 = K^2 \tag{2-10}$$

where K^2 is a constant that depends on initial conditions. If U_y and U_e are constant, equation (2-10) describes a circle in the phase-plane having γ cos λ and $\delta\lambda$ as axes, with radius K, and centered at $\left(\frac{-U_y}{\Omega}, \frac{U_e}{\Omega}\right)$. The circle, called the drift circle is the locus of the operating points defined as the instantaneous values of $\delta\lambda$ and γ cos λ. The operating point will traverse the drift circle exactly once in 24 sidereal hours. A typical drift circle is shown in Figure 2.1.

2.4 Reset Using the Drift Circle

If fixes of both latitude and azimuth are taken several hours apart, two points may be plotted in the $\delta\lambda$, γ cos λ plane. These two points alone

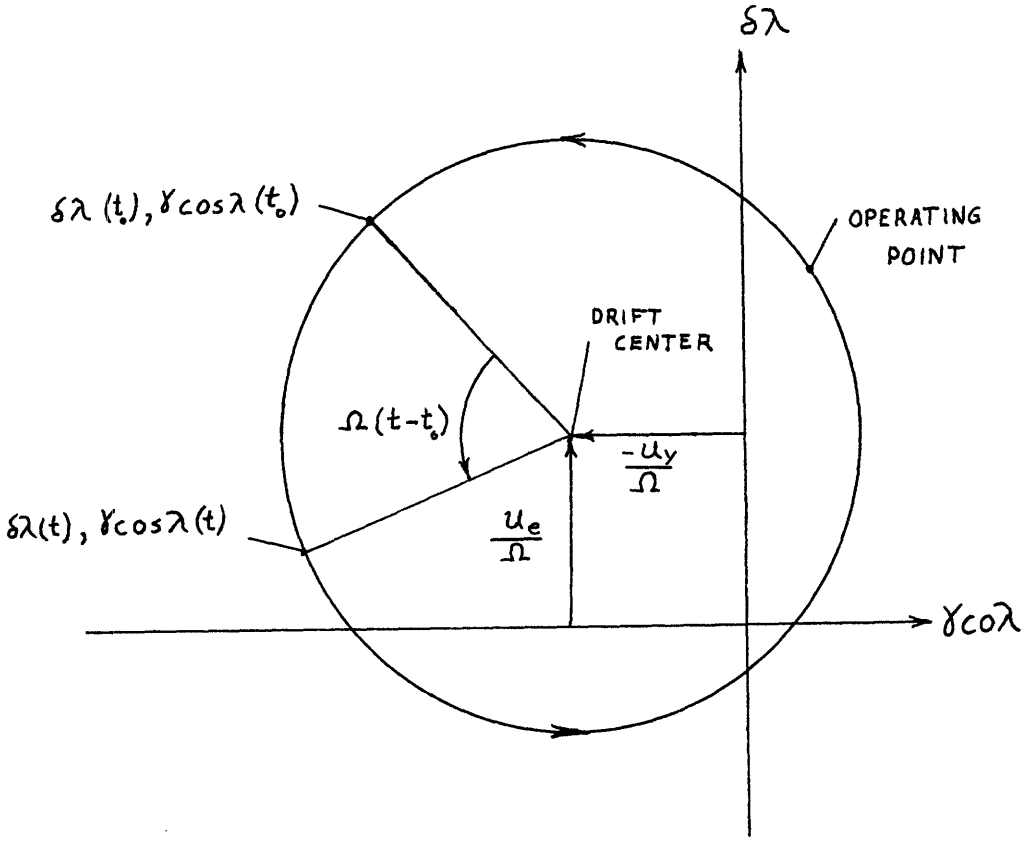

Figure 2.1 Drift Circle

will define the drift circle since the center of the circle will be on the perpendicular bisector of the points and will be the vertex of the angle $\Omega \Delta t$, where Δt is the time interval between the two fixes. The center of the circle, called the drift center, defines U_e and U_y. It should be noted at this time that inherent with this solution is the assumption that perfect fixes are obtained. If an azimuth fix is taken only once, three fixes of latitude are required to define the drift circle. If no measurement of azimuth is made, no reference is available along the $\gamma \cos \lambda$ axis. Therefore, the three latitude fixes will only define a circle relative to the $\delta\lambda$ axis. Hence only U_e will be defined, but not U_y.

If resolution of U_e into x and z components is desired, a measurement of the longtitude gyro drift, U_ℓ (in the normal four or five-gimbal mode), is required. The longtitude gyro drift can be expressed as

$$U_\ell = U_x \cos\lambda - U_z \sin\lambda \tag{2-11}$$

Multiplying the fourth equation of the matrix equation (2-1) by cos λ and subtracting from it sin λ times the sixth equation,

$$\dot{\alpha}\cos\lambda - \dot{\gamma}\sin\lambda = \delta\omega_e \sec\lambda + U_x\cos\lambda - U_z\sin\lambda \tag{2-12}$$

But, $\delta\omega_e \sec\lambda = \delta\ell$, where $\delta\ell$ is the longtitude rate error. Therefore,

$$\dot{\alpha}\cos\lambda - \dot{\gamma}\sin\lambda = \delta\dot{\ell} + U_\ell \tag{2-13}$$

Neglecting the vertical error term again, and rearranging terms,

$$\delta\dot{\ell} = -\dot{\gamma}\sin\lambda - U_\ell \tag{2-14}$$

From two successive fixes of $\delta\ell$ and γ, U_ℓ can be determined from (2-14). With U_e, the x and z components, U_x and U_z, can now be specified. Having determined the constant drifts with the aid of the circle diagram, the

gyros are torqued accordingly so as to remove the drifts.

[redacted].

CHAPTER 3

THE MODIFIED-STRAPPED-DOWN SYSTEM

3.1 Gimbaled Systems

The self-sufficient nature of inertial navigation systems is characterized by the on-board measurement of the vehicle's acceleration. Integrating this acceleration twice in the systems reference coordinate system therefore gives the navigator the desired information of vehicle's position and velocity.

The gimbals of the conventional gimbaled system perform the function of instrumenting a gyro-stabilized platform, upon which accelerometers are mounted. Because the reference coordinate system is fixed to the stable platform, the measured accelerations are already resolved in the reference system and, hence, may be used directly as inputs to the navigation equations.

3.2 The Strapped-Down System

In the gimballess, or strapped-down, configuration, the accelerometers are fixed to the vehicle. The accelerations are therefore measured with respect to a vehicle-fixed coordinate system. In certain applications, it may be more convenient to solve the system equations in the vehicle's coordinates. However, if some other reference coordinate system is used, such as an inertially-fixed or slowly rotating system, the accelerations measured in vehicle coordinates must be resolved, or transformed, into the reference coordinate system. The required transformation is generated from the rotational information of gyroscopes fixed to the vehicle. Although several other methods of representing rotational transformations have been studied for use in gimballess systems, [4] the direction cosine transformation matrix appears to be the most feasible, and will be used throughout this study.

The direction cosine matrix essentially stores the reference coordinate system. Whereas, in the gimbaled case, the reference system was stored geometrically, the transformation matrix performs an analytic storage of the reference axes.

3.3 Advantages and Disadvantages of the Strapped-Down System

The principal advantages of the strapped-down system are derived from the relative simplicity of the electromechanical equipment. Some of the more obvious advantages over a gimbaled system are 1) reduced size and weight of the electromechanical portion of the system, 2) ease of assembly, maintenance, and replacement of the inertial units, 3) reduced power consumption since no gimbal servos are required, 4) no gimbal servo stability problem and, 5) the elimination of the significant cost of gimbals.

There are, however, three major disadvantages associated with a strapped-down system. These are 1) the gyro torquing accuracy problem, 2) gyro output-axis torque and, 3) gyro cross-coupling torque problem.

3.3.1 The Torquing Accuracy Problem

In a conventional strapped-down system which uses single-degree-of-freedom gyros, angular velocity information is obtained by monitoring the torquing signals which are used to precess the gyro at the vehicle's rate. A gyro of navigational quality must be able to correctly indicate angular velocities to within a small fraction of earth rate. On the other hand, the gyro must also be capable of measuring the maximum angular velocity of the vehicle which may range from several hundreds to several thousands of earth rate units. Thus, the torquing system must simultaneously have the required range and the required accuracy. For example, if the minimum rate that must be measured is comparable to the drift of a navigational

quality gyro, [redacted] and the maximum angular velocity expected is one radian per second, a torquing accuracy of one part in a hundred million is required. Although significant advances are being made, the gyro torquing accuracy problem has remained the prohibitive factor in the use of the strapped-down configuration for high performance navigation systems.

3.3.2 The Output-Axis Torque Problem

If a gyroscope is subjected to an angular acceleration about its output-axis, an erroneous angular velocity proportional to the acceleration will be detected by the gyro. In the conventional gimballess system, this velocity error must be removed by torquing the gyro, and this involves torquing problems.

3.3.3 The Cross-Coupling Torque Problem

The cross coupling, or anisoinertia, torque is due to unequal moments of inertia of the gyro float about the spin-axis and input-axis. A torque about the output-axis results when there are simultaneous angular rates about the spin and input axes. Thus, an erroneous angular velocity is detected by the gyro which is proportional to the difference of the moments of inertia, and the simultaneous angular rates. Removal of this error in the conventional strapped-down system requires applying an equal and opposite amount of torque to the gyro, thus, further increasing the complexity of the gyro torquing system.

3.4 The Modified-Strapped-Down Inertial Navigation System

A new inertial navigation system has recently been disclosed by Charles Broxmeyer and Aldo De Simone, while both were with the MIT Instrumentation Laboratory. The new system configuration possesses some of the characteristics of gimbaled systems, and of the conventional

strapped-down systems, but does not strictly belong to either catagory. This modified-strapped-down system apparently possesses the principal advantages of both the gimbaled and gimballess systems, but does not possess their major disadvantages. The unique characteristic of this system is based on a novel inertial sensing device called the inertial reference unit.

3.4.1 The Inertial Reference Unit

The inertial reference unit is basically comprised of 1) a single-degree-of-freedom gyroscope, 2) a single-degree-of-freedom accelerometer, and 3) an output-axis compensator, which will be described below.

The gyroscope is connected to the vehicle's frame by a shaft, whose axis is coincident with the gyro's input-axis. A motor controlled by the gyro error signal is able to rotate the shaft, or equivalently, the gyro case, with respect to the vehicle. An incremental encoder mounted on the shaft, then monitors the angular motion of the gyro case relative to the vehicle. The gyro, its supporting structure, and read-out mechanism essentially forms a single-axis stable table. A schematic diagram of the device is shown in Figure 3.1.

The gyro and its supporting structure are similar to pendulous, integrating, gyro accelerometers, called PIGA's. The essential difference between the two devices is that the float of the PIGA's gyro has a mass unbalance, whereas the float of the inertial reference unit's gyro is balanced.

The gyro control loop is closed so that the gyro error signal is kept at null. That is, if the gyro senses an angular rotation about its input-axis, it will precess about its output axis, producing an error signal at the signal generator output. The error signal will then cause the motor to drive the gyro about its input axis until the error disappears. Thus, the rotation rate

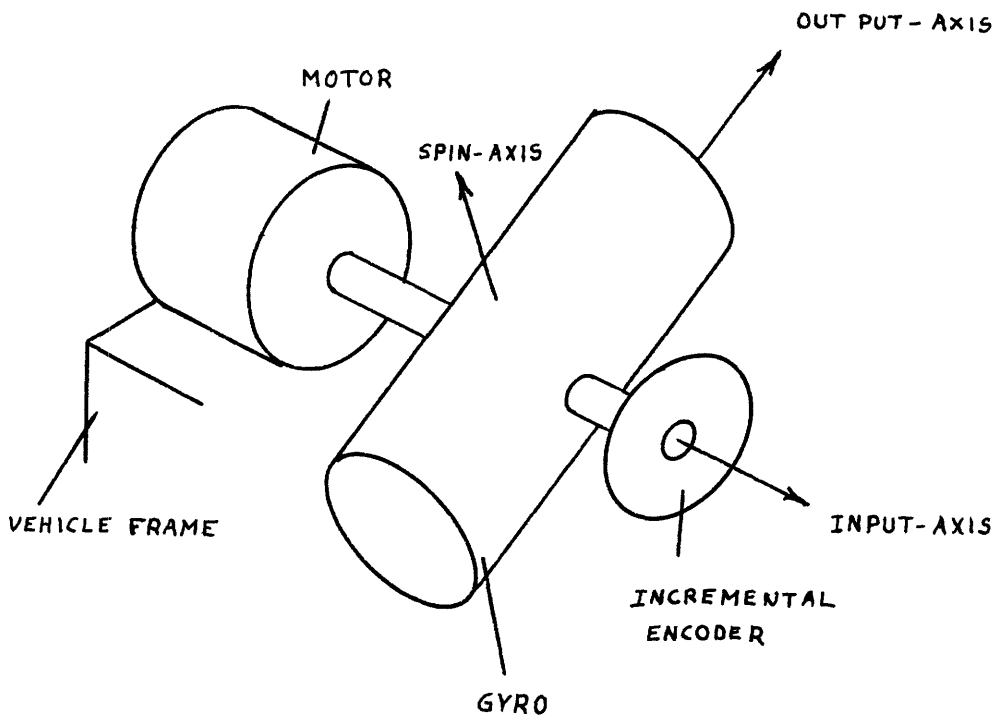

Figure 3.1 Schematic Diagram of an Inertial Reference Unit

of the gyro case measured by the incremental encoder will be equal to the component of vehicle angular velocity referred to an inertial coordinate system which exists along the gyro's input-axis.

When the inertial reference unit is mounted on the vehicle, its input-axis will always be in a fixed orientation relative to the vehicle frame. Although the output-axis and spin-axis of the gyro are free to rotate about the input-axis relative to the vehicle frame, these axes remain in a plane fixed with respect to the vehicle.

Because of the closed-loop nature of the gyro control loop and the fact that angular motion is obtained from an accurate digital encoder, the torquing accuracy problem of the conventional strapped-down system does not exist. Encoders of sufficient accuracy can be produced with state of the art techniques.

The inertial reference unit is not subject to cross-coupling torques, also. Since the device is essentially a stable platform with respect to the gyro's input-axis, simultaneous angular rates about the spin-axis and input-axis will not occur. That is, the angular rate of the gyro about its input axis referred to inertial space will always be zero.

The output-axis torque problem is also solved very nicely by the inertial reference unit. Consider a device similar in construction to the single-degree-of-freedom gyro, but having a float that is a homogeneous cylinder. This instrument, called an output-axis compensator, has signal and torque generators, and a float which is constrained by a pulse torqued-feedback loop, to remain at some null position relative to the case. If this unit is mounted rigidly to the gyro of the inertial reference unit, with the output-axes of both instruments parallel to each other, the signal applied to the torque generator of the output-axis compensator will be proportional to

the output-axis torque experienced by the gyro. Thus, with proper scaling, the torquing pulses sent to the output-axis compensator can be applied to the gyro to compensate for the output-axis torque. Of course, to be effective, the same current source must be used to torque both instruments. The accuracy or regulation of the current source has no effect on the accuracy of the compensation because of the closed loop nature of the scheme. Any changes in the level of the current source will automatically be compensated for since the number of pulses will change accordingly in order that the compensator's float remains nulled.

If a floated, pendulous accelerometer is mounted rigidly to the gyro, with their input and output axes parallel, the accelerometer will not be subjected to cross-coupling torque. The output-axis torque can be compensated for with the same output-axis compensator used with the gyro.

In summary, the inertial reference unit will 1) measure absolute incremental rotations of its case around an inertial reference axis, and 2) measure specific force information along the same axis.

A schematic diagram of an inertial reference unit is shown in Figure 3.2.

3.4.2 The Navigation System

The principal elements of the modified-strapped-down inertial navigation system are three inertial reference units and a computer. If the three inertial reference units are mounted on the vehicle with their input axes normal to each other, these axes will define a vehicle-fixed coordinate system. Each inertial reference unit will then supply angular rotation and specific force information, referred to its axis, to the computer, which will perform the necessary computations required to solve the navigation problem.

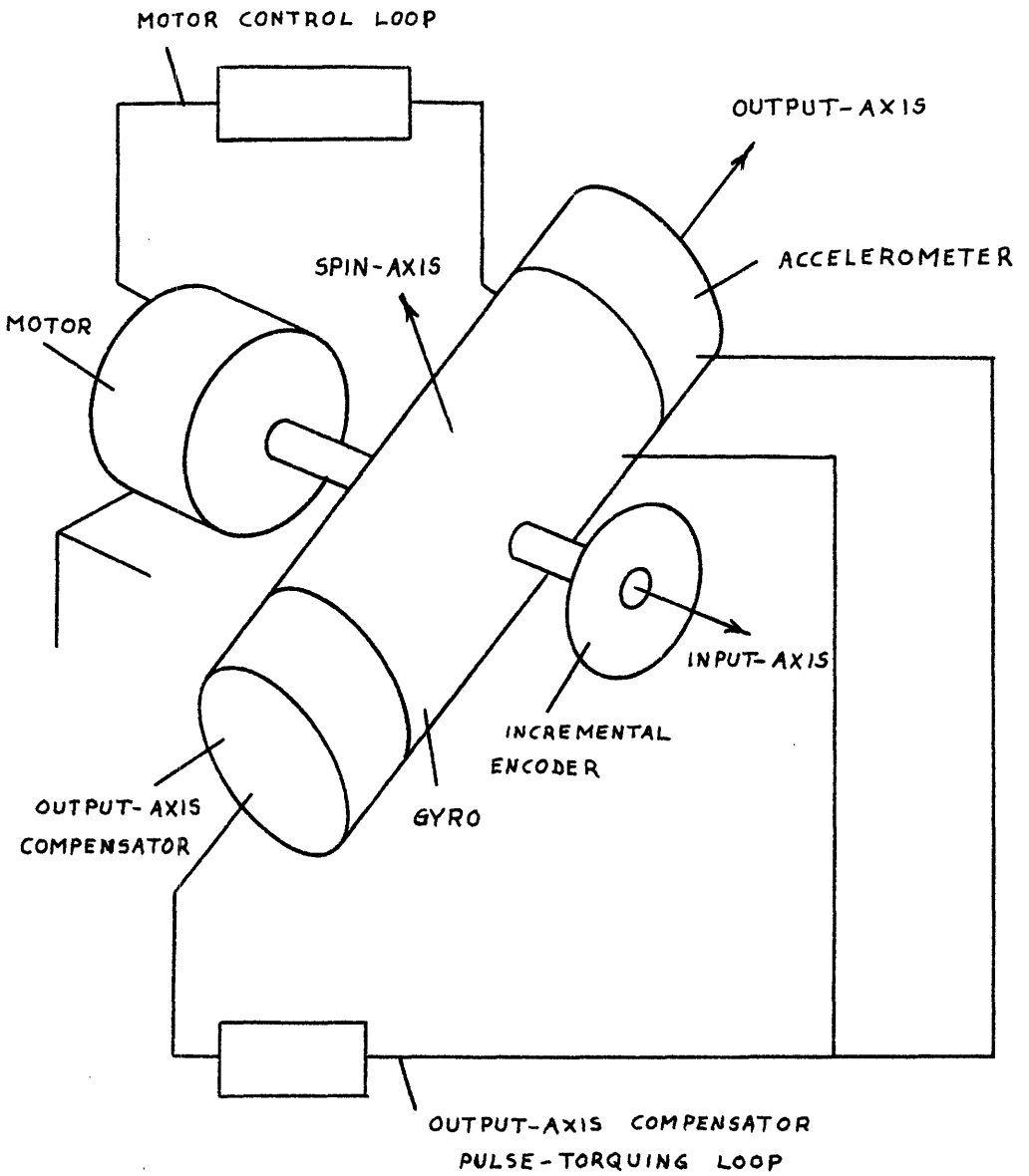

Figure 3.2 Schematic Diagram of the Complete Inertial Reference Unit

The computer may be thought of as performing two separate tasks. One of the tasks is similar to what the computer in a gimbaled system would perform. This involves the solution of the conventional navigation problem using, as inputs, specific force information referred to some indicated reference coordinate system, such as an instrumented local geographic frame. The other principal function of the computer is to generate the transformation matrix which will allow the specific force information measured in vehicle coordinates to be transformed into the indicated reference coordinate system.

The rotational matrix of direction cosines transforms specific force information from vehicle to indicated coordinate axes by,

$$f_i = C_i^v f_v \tag{3-1}$$

where $\overline{f}_i$ is the specific force vector in the indicated reference system,

$\overline{f}_v$ if the specific force measured by the inertial reference unit in vehicle axes, and

C_i^v is the transformation matrix whose elements are the direction cosines of the v-system axes with respect to the i-system axes.

The generation of C_i^v requires the solution of nine first-order differential equations, which can be expresses in matrix notation as

$$\dot{C}_i^v = C_i^v W_v - W_i C_i^v \tag{3-2}$$

W_v and W_i are the angular rate matrices of the vehicle and indicated systems, respectively, and are of the form,

$$W_v = \begin{bmatrix} 0 & -W_{vz} & W_{vy} \\ W_{vz} & 0 & -W_{vx} \\ -W_{vy} & W_{vx} & 0 \end{bmatrix} \tag{3-3}$$

where W_{vx}, W_{vy} and W_{vz} are angular rates about the v-system axes. A proof of equation (3-2) can be found in Reference (13).

W_v is thus the angular rate information measured by the vehicle mounted inertial reference units. W_i is obtained from the navigation computations based on $\overline{f}_i$. In the case where the indicated coordinate system was chosen to be an inertially non-rotating system, W_i would be zero.

Figure 3.3 shows a schematic diagram of a modified-strapped-down inertial navigation system. It has been shown that this system possesses the advantages of the conventional strapped-down system, and is not subject to the torquing accuracy problem, the output-axis torque problem, or the cross-coupling torque problem. However, if high performance over extended periods of time is required, a major problem still exists with the modified strapped-down system. This is the reset and gyro compensation problem.

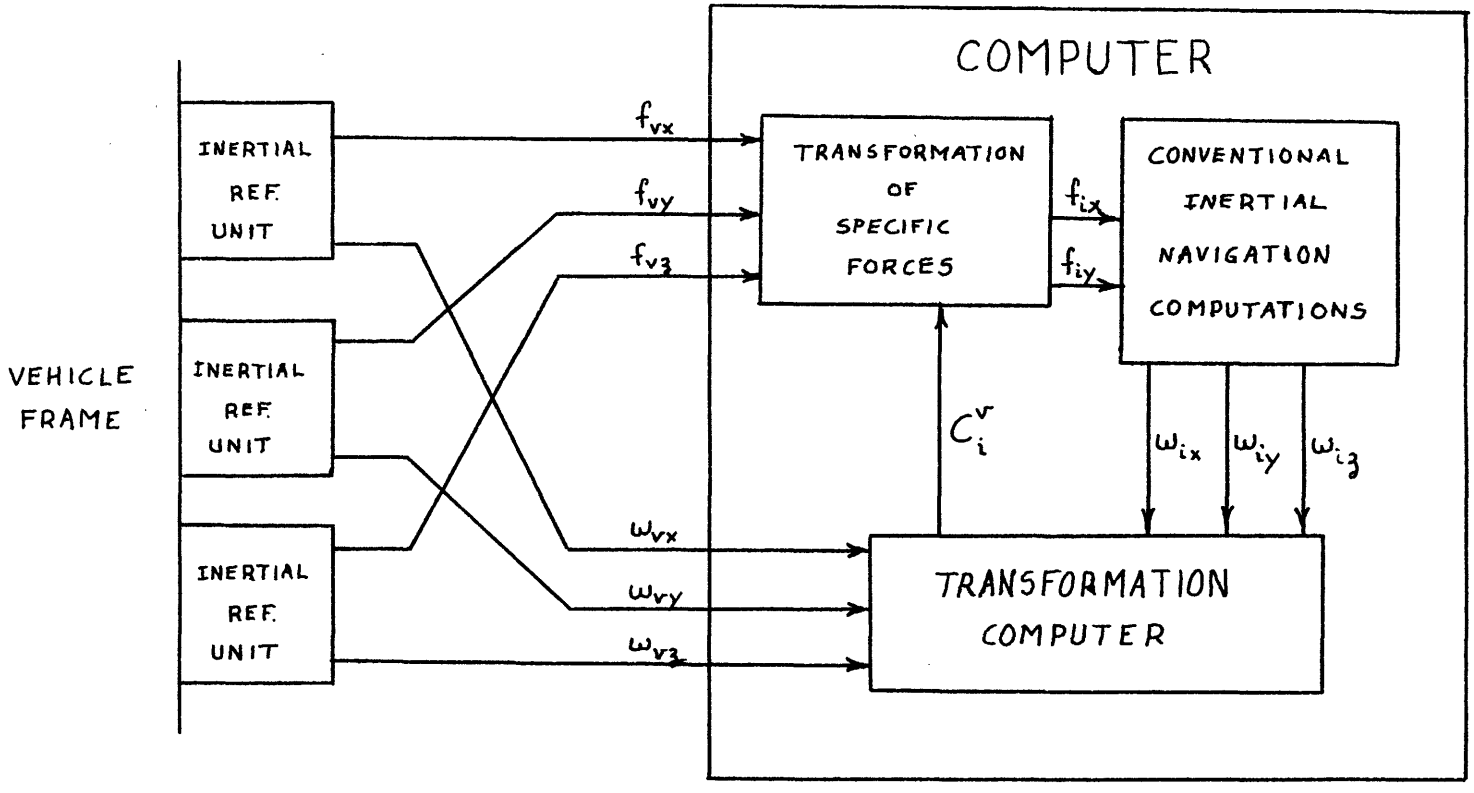

Figure 3.3 Functional Diagram of the Inertial Navigation System

CHAPTER 4

RESETTING THE STRAPPED-DOWN SYSTEM

4.1 The Problem

In gimbaled systems, relatively simple relationships between system output errors and gyro drifts exist, which do not vary with time. This is due to the stable nature of the controlled member upon which the gyros are mounted. This simplicity was demonstrated in Chapter 2, where the drift circle was used to relate various output errors to the drifts of specific gyros. That is, by simply examining the circle diagram for the last reset interval, the drifts of the equatorial and Y gyros could be determined.

However, in the case of the strapped-down system, such simple relationships do not exist. In a submarine application, a drift circle would result only if the vehicle remained level and proceeded on a fixed heading. Essentially what has happened is the inertially stable controlled member in the gimbaled system has now become unstable. Although the transformation matrix has assumed the role of the controlled member in storing a reference coordinate system, it obviously has no stabilizing effect as far as the channeling of gyro drift is concerned.

This phenomenon can be viewed more clearly if one visualizes the drifts of each of the three orthogonal gyros as being components of a "total drift" vector. Because the triad of gyros remains fixed with respect to the indicated reference coordinate system in a gimbaled system, the "total drift" vector will also remain fixed with respect to that system. Hence, the drifts of the gyros are introduced into the system in a manner which does not vary

with time. Now consider the "total drift" vector of a strapped-down system. In this case, the input axes are fixed to the vehicle. If the simple case of constant drift is assumed, we see that the "total drift" vector will be constant relative to the vehicle but will be varying its orientation as the vehicle's orientation varies relative to the indicated coordinate system. When one considers mass unbalance drifts in addition to constant drifts, the "total drift" vector also becomes a function of the vehicle's orientation relative to the gravity field. In this case, not only the orientation but the magnitude of the "total drift" vector will be varying. From the viewpoint of the system equations being solved in the indicated coordinate system, components of any of the three gyros will couple into the system to generate errors, depending on the arbitrary position of the "total drift" vector relative to the indicated coordinate system. One immediately recognizes the need for some sort of memory of the vehicle's motion if one is to solve the gyro compensation problem.

4.2 The Proposed Solution

The unique aspect of determining gyro compensation for a strapped-down system as compared to the conventional gimbaled system is that knowledge of the time history of the arbitrary vehicle motion is required.

The proposed method of solution assumes that the system output errors can be described fairly accurately as being linear functions of the gyro drifts. As such, the errors, E_i, are related to the gyro drifts, U_j, by the following equations shown below for convenience in matrix form and expressed in Laplace notation.

$$\begin{bmatrix} E_1(s) \\ E_2(s) \\ \vdots \\ E_m(s) \end{bmatrix} = \begin{bmatrix} H_{11}(s) & H_{12}(s) & \cdots & H_{1n}(s) \\ H_{21}(s) & H_{22}(s) & \cdots & H_{2n}(s) \\ \vdots & & & \vdots \\ H_{m1}(s) & H_{m2}(s) & \cdots & H_{mn}(s) \end{bmatrix} \begin{bmatrix} U_1(s) \\ U_2(s) \\ \vdots \\ U_n(s) \end{bmatrix} \tag{4-1}$$

Equation (4-1) reflects the requirement for linearity since the error, E_i, is expressed as a sum of terms, each of which is a function of a particular gyro drift, U_j. If equation (4-1) is interpreted as defining a multiple-input, multiple-output system, the elements, H_{ij}, each define a particular system transfer function. The drifts become the inputs, or forcing functions, which produce the errors as system outputs.

Transforming equation (4-1) back to the time domain, and utilizing the well-known convolution, or superposition, integral, the errors can be expressed as,

$$\begin{aligned} \epsilon_1(t) &= \int_0^t h_{11}(t-\tau)\, U_1(\tau)\, d\tau + \cdots + \int_0^t h_{1n}(t-\tau)\, U_n(\tau)\, d\tau \\ \epsilon_2(t) &= \int_0^t h_{21}(t-\tau)\, U_1(\tau)\, d\tau + \cdots + \int_0^t h_{2n}(t-\tau)\, U_n(\tau)\, d\tau \\ &\vdots \\ \epsilon_m(t) &= \int_0^t h_{m1}(t-\tau)\, U_1(\tau)\, d\tau + \cdots + \int_0^t h_{mn}(t-\tau)\, U_n(\tau)\, d\tau \end{aligned} \tag{4-2}$$

where $h_{ij}(t)$ is the inverse Laplace transform of $H_{ij}(s)$.

It thus becomes clear that it is the convolution integral which will provide a "memory" of the vehicle motion. In general usage, $h(t-\tau)$ is often termed the memory function and $(t-\tau)$ is called the memory time.

Use of equation (4-2) in determining gyro compensation proceeds as follows:

The drift terms, $U_j(\tau)$, can usually be expressed as a function of some basic constant associated with the particular drift source. Examples of these basic drift constants would be mass unbalance coefficients, compliances, or the magnitude of the component of constant drift in a gyro. It is the magnitude of each of these drift constants which must be determined such that proper compensation can be applied. In general, $U_j(\tau)$ will also be a function of vehicle motion, and hence will be time-varying. If $U_j(\tau)$ is expressed as the product of a drift constant times its corresponding time-varying function, the constant can be brought outside of the convolution integral. That is, if

$$U_j(\tau) = K_j U_j'(\tau) \tag{4-3}$$

where $U_j'(\tau)$ is the time varying function reflecting vehicle motion, then

$$\epsilon_{ij}(t) = K_j \int_0^t h_{ij}(t-\tau)\, U_j'(\tau)\, d\tau \tag{4-4}$$

If equation (4-4) is integrated in real time and evaluated at time t_l,

$$\epsilon_{ij}(t_l) = K_j \Lambda_{ij}(t_l) \tag{4-5}$$

$\Lambda_{ij}(t_\ell)$ is therefore a weighting function characterizing the error produced by the drift constant, K_j, in the time interval from t = 0 to $t = t_\ell$. $\Lambda_{ij}(t_\ell)$ is unique in the sense that it reflects the vehicle motion for that time interval.

For the case of n drift forcing functions, an error would be expressed as,

$$\epsilon_i(t_\ell) = K_1 \Lambda_{i1}(t_\ell) + K_2 \Lambda_{i2}(t_\ell) + \cdots + K_n \Lambda_{in}(t_\ell) \tag{4-6}$$

In practice, the weighting functions would be evaluated at the time that the error quality is measured. If these fix measurements occur at time, $t_o, t_1, \ldots t_\ell \ldots t_L$, we will have,

$$\begin{aligned}
\epsilon_1(t_o) &= K_1 \Lambda_{11}(t_o) + \cdots + K_n \Lambda_{1n}(t_o) \\
\epsilon_2(t_1) &= K_1 \Lambda_{21}(t_1) + \cdots + K_n \Lambda_{2n}(t_1) \\
&\vdots \qquad\qquad \vdots \qquad\qquad\qquad \vdots \\
\epsilon_m(t_L) &= K_1 \Lambda_{m1}(t_L) + \cdots + K_n \Lambda_{mn}(t_L)
\end{aligned} \tag{4-7}$$

It should be clarified that the errors, $e_i(t_\ell)$, in (4-7) need not all correspond to different system output quantities. Several of the equations of (4-7) may be fixes of the same output quantity measured at different times.

If m = n, the drift constants, K_j, may be solved for. They may be expressed in the form known as Cramer's Rule.

$$K_j = \frac{\begin{vmatrix} \Lambda_{11} \cdots \Lambda_{1,j-1} & \epsilon_1 & \cdots & \Lambda_{1n} \\ \Lambda_{21} \cdots \Lambda_{2,j-1} & \epsilon_2 & \cdots & \Lambda_{2n} \\ \vdots \quad \vdots & & & \vdots \\ \Lambda_{n1} \cdots \Lambda_{n,j-1} & \epsilon_n & \cdots & \Lambda_{nn} \end{vmatrix}}{\begin{vmatrix} \Lambda_{11} & \Lambda_{12} & \cdots & \Lambda_{1n} \\ \Lambda_{21} & \Lambda_{22} & \cdots & \vdots \\ \vdots & \vdots & & \vdots \\ \Lambda_{n1} & \cdots & \cdots & \Lambda_{nn} \end{vmatrix}} \qquad (4\text{-}8)$$

Equation (4-8) points out the fact that the designer must be careful to see that does not equal zero, in which case no solution will exist.

It is clear that this solution assumes a perfect fix. Thus, the success of the reset operations depends a great deal on the accuracy of the system which makes the fix. What this means, effectively, is that the ratio of the noise in the fix measurement to the magnitude of the actual system output errors must be small. This implies that a minimum amount of time must be allowed between resets in order that the system errors be large compared to the expected noise of the fix. If the magnitude of the indicated error is comparable to the noise level of the fix measuring system, no reset can be made. Of course, if this occurs when the fix measuring system has a low noise level, this is equivalent to the situation where no reset is required.

Once the drift constants have been determined, appropriate compensation can then be applied to the gyros to effect the removal of the drift. Such an operation is open-loop in character, and, hence, is somewhat undesirable from the engineering point of view. Either through human error, computing equipment malfunction or large fix errors, it is possible that the newly applied gyro compensation will not improve system performance, or for that matter, might even down-grade its performance. The operation is open-loop in the sense that no check is made on the effect of the computed compensation newly inserted into the system until the next fix is made, which will usually be on the order of several hours. But such is the nature of the beast. If it were possible to internally close a loop on gyro drift compensation, the reset operation would not be necessary. Thus, the reset operation can be thought of as performing a feedback function, although it is of a sampled-data nature, and possesses a low sampling-rate. The sampling rate for the inertial navigation system is, of necessity, low since high sampling rates, which would effectively be equivalent to taking a continuous fix, would make the system unnecessary. In a submarine application, the sampling rate is determined by the maximum amount of time the system will perform within specifications. The less drift that is present in the system, the longer will be the reset interval. Thus it is apparent, and this is true with all inertial navigation equipment, the limiting factor in system performance is the quality of the gyroscopes.

The remainder of the reset procedure is involved with correcting the output errors which exist when the reset is made. All outputs which have been monitored with fixes will, of course, be set to the values measured by the fix. In the situation where a reset cannot be made instantaneously at the time the fix is made, the corrections must be weighted by the effect of the time interval between fix and reset times. Quantities which were not measured can be corrected by calculating what the computed drift constants would have

contributed as errors. Thus subtraction of the computed error from the actual system output will constitute the resetting of these quantities. Resetting these "unfixed" quantities, of course, assumes that the appropriate weighting functions describing the "unfixed" output have been generated throughout the interval between resets.

In summary, the procedure to be used in resetting the strapped-down system is as follows:

1) Determine the transfer functions, $h_{ij}(t)$, relating gyro drifts to system outputs to be fixed, or to be corrected.
2) Express gyro drifts in terms of basic drift constants and time varying functions reflecting the vehicle motion, such that the constants can be factored separately into the form -- $KU_j'(\tau)$.
3) Solve the convolution integral in real time.
4) When a fix is taken, record the values of the weighting function.
5) When the number of fixed quantities equals the number of unknown drift constants, determine the values of the constants.
6) Apply gyro compensation dictated by the computed values of drift constants.
7) Correct system outputs, using fix measurements when directly applicable, or by computing error contributions based on the computed drift constants.
8) Start the next reset interval at step 3).

CHAPTER 5

THE SUBMARINE APPLICATION

5.1 The Submarine Application as an Example

The application of the modified strapped-down system as the navigator of a marine vehicle presents a realistic example where the reset operation is an important phase of successful inertial navigation. Especially in the case of missile launching submarines, where the vehicle must essentially isolate itself from the outside world, accurate performance of the navigation system over extended periods of time can only be obtained by implementing a sound reset procedure.

Besides being a very realistic example, it is also a very interesting one. Unlike some systems which may solve its equations with respect to an inertially non-rotating coordinate system, the submarine's navigation system instruments a geographic coordinate system which, in general, rotates in inertial space. The result of this rotation is reflected in the system equations by the presence of various oscillatory modes.

5.2 Derivation of the Error Matrix

The coordinate systems used in this analysis are all right-handed, orthogonal Cartesian systems with x, y, and z axes. The rotation matrix, C_n^m, expressed as,

$$C_n^m = \begin{bmatrix} C_x^x & C_x^y & C_x^z \\ C_y^x & C_y^y & C_y^z \\ C_z^x & C_z^y & C_z^z \end{bmatrix} \qquad (5\text{-}1)$$

is the matrix of transformation between the m and n coordinate systems. The elements of C_n^m are the direction cosines of the m system axes with respect to the n system axes. Therefore C_x^z would be the cosine of the angle between the z axis of the m system and the x axis of the n system. Let i refer to the indicated geographic system, t refer to the actual geographic system, and v refer to a coordinate system fixed to the vehicle.

The transformation matrix between the i and t systems can be expressed as,

$$C_t^i = C_t^v C_v^i \tag{5-2}$$

Taking the total differential of C_v^i,

$$\dot{C}_v^i = \dot{C}_t^v C_v^i + C_t^v \dot{C}_v^i \tag{5-3}$$

The term $\dot{C}_t^v$ can be expressed as a function of C_t^v and the angular velocities of the i and t systems relative to the third system which for convenience will be considered inertially non-rotating. That is

$$\dot{C}_t^v = C_t^v W_v - W_t C_t^v \tag{5-4}$$

where W_v is the vehicle's angular velocity, and

W_t is the angular velocity of the actual geographic system.

The angular velocity matrices are of the form,

$$W_m = \begin{bmatrix} 0 & -W_{mz} & W_{my} \\ W_{mz} & 0 & -W_{mx} \\ -W_{my} & W_{mx} & 0 \end{bmatrix} \tag{5-6}$$

$\dot{C}_v^i$ can also be written as,

$$\dot{C}_v^i = C_v^i W_i - W_{vm} C_v^i \tag{5-7}$$

where W_i is the computed angular velocity of the indicated frame, and

W_{vm} is the measured angular velocity of the vehicle, and hence contains drift components.

Substituting (5-4) and (5-7) into (5-3),

$$\dot{C}_t^i = C_t^v W_v C_v^i - W_t C_t^v C_v^i + C_t^v C_v^i W_i - C_t^v W_{vm} C_v^i \tag{5-8}$$

Since $C_t^v C_v^i = C_t^i$, $\dot{C}_t^i$ can be written, after rearranging terms,

$$\dot{C}_t^i = C_t^i W_i - W_t C_t^i - C_t^v (W_{vm} - W_v) C_v^i \tag{5-9}$$

But $(W_{vm} - W_v)$, the difference between the measured and actual vehicle angular velocity, is just equal to the drift, let

$$W_{vm} - W_v = \mathcal{U} \tag{5-10}$$

where

$$\mathcal{U} = \begin{bmatrix} 0 & -u_{vz} & u_{vy} \\ u_{vz} & 0 & -u_{vx} \\ -u_{vy} & u_{vx} & 0 \end{bmatrix} \tag{5-11}$$

and will be called the "total drift" vector.

Substituting (5-10) into (5-9)

$$\dot{C}_t^i = C_t^i W_i - W_t C_t^i - C_t^v \mathcal{U} C_v^i \tag{5-12}$$

If we use the identity, $C_t^v = C_t^i \, C_i^v$, equation (5-12) becomes,

$$\dot{C}_t^i = C_t^i W_i - W_t C_t^i - C_t^i (C_i^v \mathcal{U} C_v^i) \tag{5-13}$$

Premultiplying both sides of (5-13) by C_i^t,

$$C_i^t \dot{C}_t^i = C_i^t C_t^i W_i - C_i^t W_t C_t^i - C_i^t C_t^i (C_i^v \mathcal{U} C_v^i) \tag{5-14}$$

Since $C_n^m \, C_m^n = I$, the unit matrix,

$$C_i^t \dot{C}_t^i = W_i - C_i^t W_t C_t^i - C_i^v \mathcal{U} C_v^i \quad , \tag{5-15}$$

For "almost coincident" coordinate systems, it was shown in Appendix A, that C_i^t can be expressed as

$$C_i^t = \begin{bmatrix} 1 & +\gamma & -\beta \\ -\gamma & 1 & +\alpha \\ +\beta & -\alpha & 1 \end{bmatrix} = I + A \tag{5-16}$$

In books treating matrices[14] it is shown that the inverse of a rotation matrix between two Cartesian coordinate systems is equal to its transpose. Therefore,

$$C_t^i = C_{iT}^t = \begin{bmatrix} 1 & -\gamma & \beta \\ \gamma & 1 & -\alpha \\ -\beta & \alpha & 1 \end{bmatrix} = I - A \tag{5-17}$$

Differentiating (5-17) with respect to time,

$$\dot{C}_t^i = \begin{bmatrix} 0 & -\dot{\gamma} & \dot{\beta} \\ \dot{\gamma} & 0 & -\dot{\alpha} \\ -\dot{\beta} & \dot{\alpha} & 0 \end{bmatrix} = -\dot{A} \tag{5-18}$$

Therefore,

$$C_i^t \dot{C}_t^i = (I + A)(-\dot{A}) \tag{5-19}$$

If second order terms are neglected

$$C_i^t \dot{C}_t^i = -\dot{A} \tag{5-20}$$

Equation (5-15) can now be written as

$$-\dot{A} = W_i - C_i^t W_t C_t^i - C_i^v U C_v^i \tag{5-21}$$

The similarity transformation for anti-symmetric matrices can be applied to (5-21) to yield the following vector equation,

$$-\overline{\dot{A}} = \overline{W_i} - C_i^t \overline{W_t} - C_i^v \overline{U} \tag{5-22}$$

Expressed in component form,

$$\begin{aligned} \dot{\alpha} &= \omega_{ix} - \omega_{tx} - \gamma\omega_{ty} + \beta\omega_{tz} - U_X \\ \dot{\beta} &= \omega_{iy} - \omega_{ty} - \alpha\omega_{tz} + \gamma\omega_{tx} - U_Y \\ \dot{\gamma} &= \omega_{iz} - \omega_{tz} - \beta\omega_{tx} + \alpha\omega_{ty} - U_Z \end{aligned} \tag{5-23}$$

where U_X, U_Y, and U_Z are the components of drift transformed from vehicle to indicated coordinate systems.

By following a similar development to that used in Appendix A for the navigation error equations, and again assuming a stationary vehicle, the following error matrix shown as (5-24) will result.

In addition to the drift terms of (5-24) being functions of vehicle motion, the difference between (5-24) and (2-1) is the appearance of a minus sign before the drift column matrix of (5-24). A physical interpretation of this minus sign can be obtained by considering the following:

$$\begin{bmatrix} \delta\dot{\omega}_n \\ \delta\dot{\omega}_e \\ \delta\dot{\lambda} \\ \dot{\alpha} \\ \dot{\beta} \\ \dot{\gamma} \end{bmatrix} = \begin{bmatrix} 0 & -2\Omega\sin\lambda & 0 & 0 & g/R & 0 \\ 2\Omega\sin\lambda & 0 & 0 & -g/R & 0 & 0 \\ 1 & 0 & 0 & 0 & 0 & 0 \\ 0 & 1 & -\Omega\sin\lambda & 0 & -\Omega\sin\lambda & 0 \\ -1 & 0 & 0 & \Omega\sin\lambda & 0 & \Omega\cos\lambda \\ 0 & -\tan\lambda & -\Omega\cos\lambda & 0 & -\Omega\cos\lambda & 0 \end{bmatrix} \begin{bmatrix} \delta\omega_n \\ \delta\omega_e \\ \delta\lambda \\ \alpha \\ \beta \\ \gamma \end{bmatrix} - \begin{bmatrix} 0 \\ 0 \\ 0 \\ U_x \\ U_y \\ U_z \end{bmatrix}$$

(5-24)

If a gimbaled system is operating in the three-gimbal mode, the input axes of the gyros mounted on the stable member will define the indicated coordinate system. If the "total drift" vector of the three gyros is defined as being positive, the stable member, and hence the indicated coordinate system, will rotate in a positive sense. That is, the stable member will "follow" the gyro drift. However, in the case of the strapped-down system, a positive "total drift" vector will cause the transformation computer to interpret the drift as a positive angular velocity of the vehicle with respect to the indicated coordinate system. Thus the indicated coordinate system will appear to rotate in a negative sense. In other words, the indicated coordinate system will rotate "away" from the actual drift direction. Hence, the appearance of the minus sign.

5.3 The Error Transfer Functions

Comparison of equations (5-22) and (5-23) shows that,

$$\begin{aligned} u_x &= C_x^x u_{vx} + C_x^y u_{vy} + C_x^3 u_{v3} \\ u_y &= C_y^x u_{vx} + C_y^y u_{vy} + C_y^3 u_{v3} \\ u_z &= C_3^x u_{vx} + C_3^y u_{vy} + C_3^3 u_{v3} \end{aligned} \qquad (5\text{-}25)$$

where the C's are the elements of the transformation matrix C_i^v, which is instrumented in the system by the transformation computer. The u_v's are the gyro drifts measured about the gyro input axes.

By developing the circle diagram equations as was done in Chapter 2, and by taking into account the minus sign before the drift terms, the following equations will result.

$$\dot{\gamma}\cos\lambda = -\Omega\,\delta\lambda - u_x \sin\lambda - u_z \cos\lambda \qquad (5\text{-}26)$$

$$\delta\dot{\lambda} = \Omega\gamma\cos\lambda - u_y \qquad (5\text{-}27)$$

$$\delta\dot{l} = -\dot{\gamma}\sin\lambda + u_x\cos\lambda - u_z \sin\lambda \qquad (5\text{-}28)$$

Multiplying (5-26) by tan λ,

$$\dot{\gamma} \sin\lambda = -\Omega \tan\lambda \, \delta\lambda - u_x \frac{\sin^2\lambda}{\cos\lambda} - u_z \sin\lambda \tag{5-29}$$

Substituting (5-29) into (5-28),

$$\begin{aligned} \dot{\delta\ell} &= \Omega \tan\lambda \, \delta\lambda + u_x \left(\cos\lambda + \frac{\sin^2\lambda}{\cos\lambda}\right) \\ &= \Omega \tan\lambda \, \delta\lambda + u_x \sec\lambda \end{aligned} \tag{5-30}$$

Equations (5-26), (5-27), and (5-30) can be used to construct the following flow graph, expressed in Laplace notation.

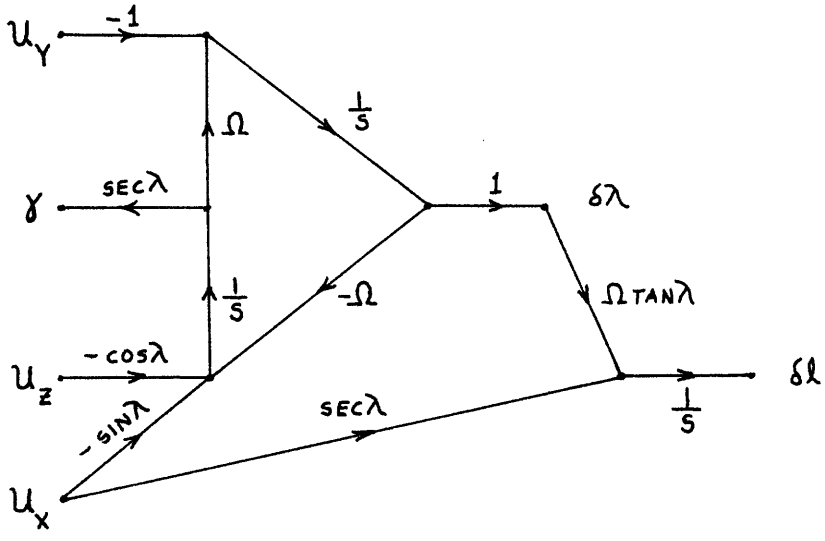

Figure 5-1 Flow Diagram of the Error Equations

The transfer functions between the errors and the drifts, as determined from the flow graph, are:

$$\frac{\delta\lambda(s)}{u_x(s)} = -\sin\lambda \frac{\Omega}{s^2 + \Omega^2} \tag{5-31}$$

$$\frac{\delta\lambda(s)}{U_Y(s)} = -\frac{s}{s^2+\Omega^2} \tag{5-32}$$

$$\frac{\delta\lambda(s)}{U_Z(s)} = -\cos\lambda\,\frac{\Omega}{s^2+\Omega^2} \tag{5-33}$$

$$\frac{\gamma(s)}{U_X(s)} = -\tan\lambda\,\frac{s}{s^2+\Omega^2} \tag{5-34}$$

$$\frac{\gamma(s)}{U_Y(s)} = \sec\lambda\,\frac{\Omega}{s^2+\Omega^2} \tag{5-35}$$

$$\frac{\gamma(s)}{U_Z(s)} = -\frac{s}{s^2+\Omega^2} \tag{5-36}$$

$$\frac{\delta\ell(s)}{U_X(s)} = \frac{\cos\lambda}{s} + \sin\lambda\tan\lambda\,\frac{s}{s^2+\Omega^2} \tag{5-37}$$

$$\frac{\delta\ell(s)}{U_Y(s)} = -\tan\lambda\,\frac{\Omega}{s^2+\Omega^2} \tag{5-38}$$

$$\frac{\delta\ell(s)}{U_Z(s)} = \sin\lambda\,\frac{s}{s^2+\Omega^2} - \frac{\sin\lambda}{s} \tag{5-39}$$

These transfer functions correspond to the $H_{ij}(s)$ terms introduced in equation (4-1) as system transfer functions. Transformation of these functions into the time domain yield system impulse responses which describe simple integrators or harmonic oscillators with natural frequencies equal to earth's rate, as shown below.

$$h_{\delta\lambda,U_X}(t) = -\sin\lambda\sin\Omega t \tag{5-31^1}$$

$$h_{\delta\lambda,U_Y}(t) = -\cos\Omega t \tag{5-32^1}$$

$$h_{\delta\lambda,U_Z}(t) = -\cos\lambda\sin\Omega t \tag{5-33^1}$$

$$h_{\gamma,u_x}(t) = -\tan\lambda \cos\Omega t \qquad (5\text{-}34^1)$$

$$h_{\gamma,u_y}(t) = \sec\lambda \sin\Omega t \qquad (5\text{-}35^1)$$

$$h_{\gamma,u_z}(t) = -\cos\Omega t \qquad (5\text{-}36^1)$$

$$h_{\delta\ell,u_x}(t) = \cos\lambda \int(\ )\,dt + \sin\lambda \tan\lambda \cos\Omega t \qquad (5\text{-}37^1)$$

$$h_{\delta\ell,u_y}(t) = -\tan\lambda \cos\Omega t \qquad (5\text{-}38^1)$$

$$h_{\delta\ell,u_z}(t) = \sin\lambda \cos\Omega t - \sin\lambda \int(\ )\,dt \qquad (5\text{-}39^1)$$

5.4 Drift Forcing Functions

Extensive analysis of single-degree-of-freedom gyroscopes has been performed.[15] [16] [17] [18] Some studies included investigations of gyroscope behaviour when the device is subjected to various environmental conditions[19] [20] [21] which are similar to a strapped-down environment, i.e. linear and angular vibrations. Gyro drift can be considered as being comprised of four principal components; 1) a nonacceleration sensitive, or constant, component caused primarily by flex-lead and microsyn-reaction torques, 2) acceleration sensitive, or mass unbalance, torques due to moments along the input-axis and open-axis, 3) acceleration-squared sensitive torques caused by compliances of the gyro inner package, and 4) a random component. Reset data from submarine inertial navigation systems at sea indicate that the assumption of constant drift, and consequently the use of a circle-diagram in resetting, is well justified. Because the gyros remain in essentially a fixed orientation relative to the gravity field and are not subjected to large translational acceleration, the "constant" component of drift determined by the circle

diagram may well include mass unbalance contributions which are relatively constant. In a strapped-down environment, these mass unbalance torques will undoubtably become a major source of drift. In the following analysis, only constant and mass unbalance drifts will be considered. In a later section, compensation for other drift sources will be discussed.

Let the vehicle axes defined by the three orthogonal gyro input axes be such that the x-axis points forward along the roll axis of the vehicle, the y-axis is along the pitch axis to star-board, and the z-axis is down, along the yaw axis.

The transformation matrix, C_i^v, will transfer specific force measurements in these vehicle coordinates to the indicated geographic coordinate system. It thus provides an analytical storage of the indicated system. If the vehicle's axes are perfectly aligned with the true geographic axes, and the transformation matrix is correct, it will be a unit matrix.

5.4.1 Constant Drift

In Section 5.3 it was shown that the drift forcing functions, U_X, U_Y, and U_Z could be expressed in terms of the elements of the direction cosine transformation matrix and the drift measured by the gyros. The equations are shown below for convenience.

$$\begin{aligned} U_x &= C_x^x u_{vx} + C_x^y u_{vy} + C_x^3 u_{v3} \\ U_y &= C_y^x u_{vx} + C_y^y u_{vy} + C_y^3 u_{v3} \\ U_z &= C_3^x u_{vx} + C_3^y u_{vy} + C_3^3 u_{v3} \end{aligned} \tag{5-25}$$

In the simple case of constant drifts, u_k, the corresponding drift forcing functions are identical to (5-25) where now, $u_v = u_k$. That is

$$\begin{bmatrix} u_x \\ u_y \\ u_z \end{bmatrix} = \begin{bmatrix} & C_i^v & \end{bmatrix} \begin{bmatrix} u_{kx} \\ u_{ky} \\ u_{kz} \end{bmatrix} \tag{5-40}$$

5.4.2 Mass Unbalance Drift

In Chapter 3 it was observed that although the plane defined by a gyro's output and spin axes remained fixed relative to the vehicle, the axes themselves were free to rotate about the input-axis. Therefore, there exists an arbitrary choice as to how the output axis will be initially positioned. It should be noted that after some arbitrary motion, if the vehicle axes return to their original orientation, the output axis will not necessarily be at its original position. The angular displacement discrepancy is a result of the non-additive property of finite rotation angles. This phenomenon can be described as a coning effect, although "coning" drift does not occur in the modified strapped-down system because angular rotations are measured about the instantaneous gyro input-axes.

For the present, let us assume that the X and Y gyros have their output axes vertical, and the output-axis of the Z gyro is horizontal, initially.

Expressions for mass unbalance drifts in vehicle coordinates will first be determined. Then use of equation (5-25) will put these drifts in the desired form.

Because mass unbalance torque about the output-axis of the gyro is a function of the gravity field, an expression for the gravity vector in vehicle

coordinates is required. Ideally, the gravity vector, $\bar{g}_o$, would be given in vehicle coordinates by,

$$\bar{g}_v = C_v^t \bar{g}_o \tag{5-41}$$

where C_v^t is the transformation matrix between the actual geographic and vehicle systems, and $\bar{g}_o$, in geographic coordinates, is,

$$\bar{g}_o = \begin{bmatrix} 0 \\ 0 \\ g_o \end{bmatrix} \tag{5-42}$$

The matrix C_v^t is never known exactly by the system, although its attempt to instrument C_v^t results in C_v^i, (C_v^i being the transpose of C_i^v). Since, for a system with reasonable performance, the angle errors between the t and i systems are of the order of a couple of minutes of arc, $\bar{g}_v$ can be expressed fairly accurately by,

$$\bar{g}_v = C_v^i \bar{g}_o \tag{5-43}$$

where,

$$C_v^i = C_{iT}^v = \begin{bmatrix} C_x^x & C_y^x & C_3^x \\ C_x^y & C_y^y & C_3^y \\ C_x^3 & C_y^3 & C_3^3 \end{bmatrix} \tag{5-44}$$

If $\bar{i}_{vx}$, $\bar{i}_{vy}$, and $\bar{i}_{vz}$ denote unit matrices along the vehicle coordinates, using (5-42), (5-43), and (5-44),

$$\bar{g}_v = g_o \left(C_3^x \bar{i}_{vx} + C_3^y \bar{i}_{vy} + C_3^3 \bar{i}_{v3} \right) \tag{5-45}$$

Consider a mass unbalance moment, U_{IA}, along the input axis. If $\bar{i}_{IA}$ and $\bar{i}_{OA}$ are unit vectors along the input and output axes, respectively, the resultant torque about the output-axes is,

$$\tau_{IA} = U_{IA} (\bar{i}_{IA} \times \bar{g}_v) \cdot \bar{i}_{OA} \tag{5-46}$$

Similarly, the torque about the output-axis due to a mass unbalance along the spin-axis, SA, is,

$$\tau_{SA} = U_{SA} (\bar{i}_{SA} \times \bar{g}_v) \cdot \bar{i}_{OA} \tag{5-47}$$

Since the input axes define the vehicle coordinates, $\bar{i}_{IA} = \bar{i}_V$. The vector $\bar{i}_{OA}$ and the unit vector along the spin-axis, $\bar{i}_{SA}$, can be defined by rotation angles about the input-axis, the two being displaced from each other by 90 degrees. Let the rotation angles, called θ_x, θ_y, and θ_z and corresponding to the X, Y, and Z gyros, be defined as the angles of the output axes relative to some initial reference direction. For simplicity, let us assume that when the vehicle's axes are initially aligned with the geographic axes, the output axes of the X and Y gyros are vertical and the Z gyro output-axis is along the $\bar{i}_{vy}$ direction. In this case, θ will just be equal to the integral of the rate measured by the gyro, thereafter.

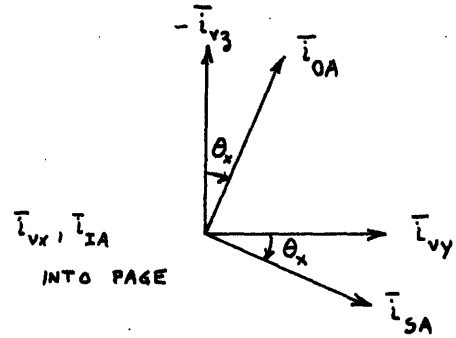

Figure 5-2 Definition of θ_x

From Figure 5-2

$$\begin{aligned} \bar{\imath}_{OAx} &= \sin\theta_x\, \bar{\imath}_{vy} - \cos\theta_x\, \bar{\imath}_{v3} \\ \bar{\imath}_{SAx} &= \cos\theta_x\, \bar{\imath}_{vy} + \sin\theta_x\, \bar{\imath}_{v3} \\ \bar{\imath}_{IAx} &= \bar{\imath}_{vx} \end{aligned} \tag{5-48}$$

Using (5-45), (5-46), (5-47), and (5-48), the torque about the output-axis of the x gyro due to IA mass unbalance is,

$$\tau_{IAx} = -g_o U_{IAx} (C_3^3 \sin\theta_x + C_3^y \cos\theta_x) \tag{5-49}$$

and the torque due to spin-axis mass unbalance is,

$$\tau_{SAx} = g_o U_{SAx} C_3^x \tag{5-50}$$

Similarly, for the Y and Z gyros,

$$\tau_{IAy} = g_o U_{IAy} (C_3^x \cos\theta_y - C_3^3 \sin\theta_y) \tag{5-51}$$

$$\tau_{SAy} = g_o U_{SAy} C_3^y \tag{5-52}$$

$$\tau_{IA3} = g_o U_{IA3} (C_3^x \cos\theta_3 + C_3^y \sin\theta_3) \tag{5-53}$$

$$\tau_{SA3} = g_o U_{SA3} C_3^3 \tag{5-54}$$

Expressed as drifts measured at the gyro input axes,

$$\begin{aligned} u_{mx} &= \frac{g_o}{H} (U_{IAx} (-C_3^y \cos\theta_x - C_3^3 \sin\theta_x) + U_{SAx} C_3^x) \\ u_{my} &= \frac{g_o}{H} (U_{IAy} (C_3^x \cos\theta_y - C_3^3 \sin\theta_y) + U_{SAy} C_3^y) \\ u_{m3} &= \frac{g_o}{H} (U_{IA3} (C_3^x \cos\theta_3 + C_3^y \sin\theta_3) + U_{SA3} C_3^3) \end{aligned} \tag{5-55}$$

where H is the angular momentum of the gyro spin wheel.

The total drift forcing function will therefore be,

$$\begin{bmatrix} u_x \\ u_y \\ u_z \end{bmatrix} = \begin{bmatrix} & C_i^v & \end{bmatrix} \begin{bmatrix} u_{kx} + u_{mx} \\ u_{ky} + u_{my} \\ u_{kz} + u_{mz} \end{bmatrix} \tag{5-56}$$

Thus, the drift forcing functions can be expressed as functions of C_i^v, θ-angles, U_k's, U_{SA}'s, and U_{IA}'s.

5.5 Determination of the Drift Constants

As an example of the use of the convolution integral in providing weighting functions of past vehicle motion, consider the latitude error produced by a constant drift, u_{ky}, in the Y-gyro. For further simplicity, let us assume that the vehicle is operating near the equator, in which case $\lambda = 0$. Equations (4-2), (5-32), (5-33), and (5-40) give, for the component of latitude error produced by u_{ky},

$$\Delta\delta\lambda(t) = -\int_0^t \cos\Omega(t-\tau)\, C_y^y u_{ky}\, d\tau - \int_0^t \sin\Omega(t-\tau) C_3^y u_{ky}\, d\tau \tag{5-57}$$

To express equation (5-57) in a form more suitable for real-time solution by the system computer, use of trigonometric identities for the sine and cosine of the difference of two angles will give,

$$\Delta\delta\lambda(t) = -u_{ky}\left[\cos\Omega t \int_0^t \cos\Omega\tau\, C_y^y\, d\tau + \sin\Omega t \int_0^t \sin\Omega\tau\, C_y^y\, d\tau + \sin\Omega t \int_0^t \cos\Omega\tau\, C_3^y\, d\tau - \cos\Omega t \int_0^t \sin\Omega\tau\, C_3^y\, d\tau\right] \tag{5-58}$$

where u_{ky} has been brought outside the integrals, since it has been assumed to be a constant.

With the computer's integrators set to zero at the start of the reset interval (t = 0), the integrals of (5-58) are solved continuously in real-time. When a fix on latitude is made at some time t_o, the bracketed term of (5-58) is evaluated and recorded. This term, which has now been recorded as a constant, is the weighting function on how much error u_{ky} has contributed in the latitude output. If $\Delta\delta\lambda$ (t) is the error contribution,

$$\Delta\delta\lambda(t_o) = u_{ky}\,\Lambda(t_o) \tag{5-59}$$

where $\Lambda(t_o)$ is the weighting function. Thus, if all gyro drift constants are accounted for, the latitude error determined by the fix measurement would be expressed as a sum of $\Delta\delta\lambda(t_o)$ components similar to (5-59). That is, for n unknown drift constants,

$$\delta\lambda(t_o) = \sum_{i=0}^{n} u_i\,\Lambda_i(t_o) \tag{5-60}$$

Weighting functions for longitude and azimuth errors must also be computed in the system. The expressions for the weighting functions of latitude error when constant and mass unbalance drifts are assumed, and expressions for longitude and azimuth errors when only constant drifts are assumed are shown in Appendix B.

Since each fix of either latitude, longitude or azimuth results in one equation containing n unknowns, corresponding to the n unknown drift constants, a total of n fixed quantities is required for the evaluation of the n unknowns.

In general, fixes of latitude, longitude and azimuth are available. Depending on vehicle position or meteorological conditions, such as cloud cover or sea state, perhaps only one or two of these quantities will be available. Because azimuth measurements take a relatively long fix time and

require vehicle exposure above the surface, usually fixes of only latitude and longitude are made using the Loran system. Such measurements can be made fairly quickly and do not require serious vehicle exposure.

It should be mentioned here that the interval between fixes must not be too short. If the same quantity is fixed too soon, the weighting functions and the measured errors will not have changed very much since the last fix was taken, and no new information will have been obtained by the fix. Stated another way, two of the n fix equations will be dependent, thus making the determinant in the denominator of (4-8) zero.

5.6 The Reset Operation

The reset operation basically involves 1) the correction of system output errors which may exist, and 2) the application of proper gyro compensation in order that the tendency for the growth of output errors is reduced.

After the required number of fixes have been obtained, the drift constants can be calculated. A reset is usually made immediately after the last fix has been taken so that the fix measurements may be used directly to correct the fixed output quantities. Outputs which have not been fixed are corrected by a simple calculation involving the computed drift constants and the weighting functions for the particular quantity being corrected. This is essentially a reversal of the procedure for determining the drift constants, since now the drift constants are known and the error is unknown. Subtraction of the computed error from the system output value constitutes the correction of the unfixed quantity.

At reset, the computed values of the drift constants are used in generating torquing signals to the gyros. The computer instruments equation (5-55) using the new values of U_{IA} and U_{SA}. Adding these mass unbalance torquing values to the computed constant drift values, the computer controls, through pulse torquing, the required compensation to each gyro.

When these reset operations have been done, the weighting function integrators are zeroed and the next reset interval is begun.

5.7 Discussion

Reference to Appendix B shows that a sizeable amount of computing equipment is required to perform the necessary reset computations. However, this is not surprising since the proposed reset solution inherently involves the storage of information. Such an operation usually means the addition of more computing machinery.

Because a submarine remains fairly level, especially when it is submerged, a possibility exists for making several simplifications in the equations which must be solved. This characteristic of having essentially planar motion means that cross-coupling terms between the x-y plane and the z-axis will be small. In terms of the transformation matrix, the elements C_z^x, C_z^y, C_x^z, and C_y^z will be small compared to the others. These simplifications will be discussed more fully in the following chapter.

If constant and mass unbalance drifts are assumed, nine drift constants must be solved for. Their evaluation, therefore, requires a total of nine fixed quantities. In the usual case where only latitude and longitude fixes are available, five fix intervals are needed. Although the number may appear to be large, it must be recognized that the drift of all three gyros will be determined with only latitude and longitude information. In the gimbaled case, no compensation to the Y gyro can be applied without an azimuth fix.

If only constant drift is assumed, only one fix interval will be required if azimuth, latitude, and longitude are measured, compared to the minimum of two fix intervals for the gimbaled case. The possibility of assuming constant drift in a strapped-down system is not unrealistic since past experience with single-degree-of-freedom gyros has shown that only a slow change, or "creeping",

in the mass unbalance coefficients takes place as time passes. If this proves to be the case in a strapped-down application, the first few resets would be performed assuming constant and mass unbalance drifts. After the mass unbalances have been fairly well determined, resets could be based on the constant drift model, with only occasional mass unbalance checks being performed thereafter. The advantage of being able to compensate all three gyros with only one fix interval is great. Compared to gimbaled system reset performance, it either will allow the fix interval to be increased substantially with little loss in system performance, or it will improve system performance if reset intervals comparable to those used with gimbaled systems is maintained. Of course the effectiveness of the constant gyro drift model with slowly varying mass unbalance in a strapped-down environment is questionable at this time and can only be determined by extensive experiments.

The problem of compensating for compliance drifts appears to be a formidable one. In addition to being functions of vehicle orientation, the effect of angular and translational accelerations must be accounted for. Such drifts are neglected in gimbaled systems since the stable platform renders them negligible. Although compliance torques can be analytically described in terms of compliance constants, in addition to the previously mentioned quantities, the complexity and sheer number of computations required to determine these constants by the method of this thesis precludes such a solution. It would appear that the most feasible way of attacking this problem, should compliance drifts prove to be a major error source, would be to improve the inertial device itself.

Random drift, by its very nature, presents a difficult problem. Even in the simple case of a gimbaled system, resets for random drift are not attempted, although various studies have been directed towards this end.

The major problem appears to be a lack of reliable statistical data with which to describe the random behavior. This is due to the fact that little concern has been focused on random drift, since it has been found to be small compared to the constant component. Perhaps all the designer can do on this account is to hope that the random drift component will also be small in the strapped-down application.

CHAPTER 6

SIMPLIFICATIONS AND SIMULATIONS OF THE SUBMARINE RESET

6.1 Simplifications

The motion of a submarine relative to its local geographic coordinate system is not completely arbitrary. Although the vehicle's heading may be arbitrary, the vehicle remains relatively level throughout its cruise. That is, its motion is effectively restricted to being planar, with respect to the geographic system. Moreover, when submerged, list can be controlled very closely. The possibility therefore exists for simplifying the reset computations without appreciably reducing the effectiveness of the reset operation. The simplification of the three-dimensional problem to the two-dimensional one involves setting the elements C_z^x, C_z^y, C_x^z, C_y^z of the transformation matrix to zero and C_z^z to one. This reduces the direction cosine matrix to a two-by-two matrix.

In this chapter, a study is made to determine the effectiveness of resets performed under the assumption that vehicle motion is planar. The procedure to be used is the following:

1) Determine a realistic model of submarine motion from experimental data.
2) Simulate, on a digital computer, the reset operation with and without simplifications. In the simplified case, $C_z^x = C_z^y = C_x^z = C_y^z = 0$ and $C_z^z = 1$.
3) Evaluate the effectiveness of the reset using simplifications.

A secondary, but nevertheless important, reason for making these simulations is that they will provide a good check on the general reset solution

proposed by this thesis. If the vehicle's axes are initially aligned with the geographic axis, and are then only allowed to oscillate about this orientation, the errors generated in the strapped-down system should be similar to those generated by a gimbaled system. A comparison would therefore provide a check on the correctness of the strapped-down reset equations.

6.2 Submarine Motion

The U. S. Navy Department's David Taylor Model Basin has been an ideal source for experimental data on submarine motion. In a series of reports,[22] a spectrum analysis of the motion of the U.S.S. Raton (SSR270) during sea trials is presented. Figure 6.1 shows a representative spectrum of roll motion when proceeding submerged in a state 5 sea. Pitch and roll motion spectra for submerged, surfaced, or snorkeling conditions all have the same general profile, where most of the energy is concentrated at approximately 0.5 radians per second. The major difference between the spectra, as far as this study is concerned, is that the area under the spectra varied. For the purposes of this investigation, the spectrum profile shown in Figure 6.1 can be used to describe both pitch and roll motion. The mean square value, which is equal to the area under the spectrum, will, of course, vary.

6.2.1 The Model

A major consideration concerning the choice of a model which describes vehicle motion is the amount of computer time required to simulate realistic time intervals between resets. We have seen that the evaluation of the error weighting functions involves the integration process. If the function being integrated is a continuous function, as would be the actual case of the varying direction cosines, the integration operation on a general purpose digital computer would involve a time consuming iterative process such as a Runge-Kutta technique. When one considers that the period of the submarines motion is

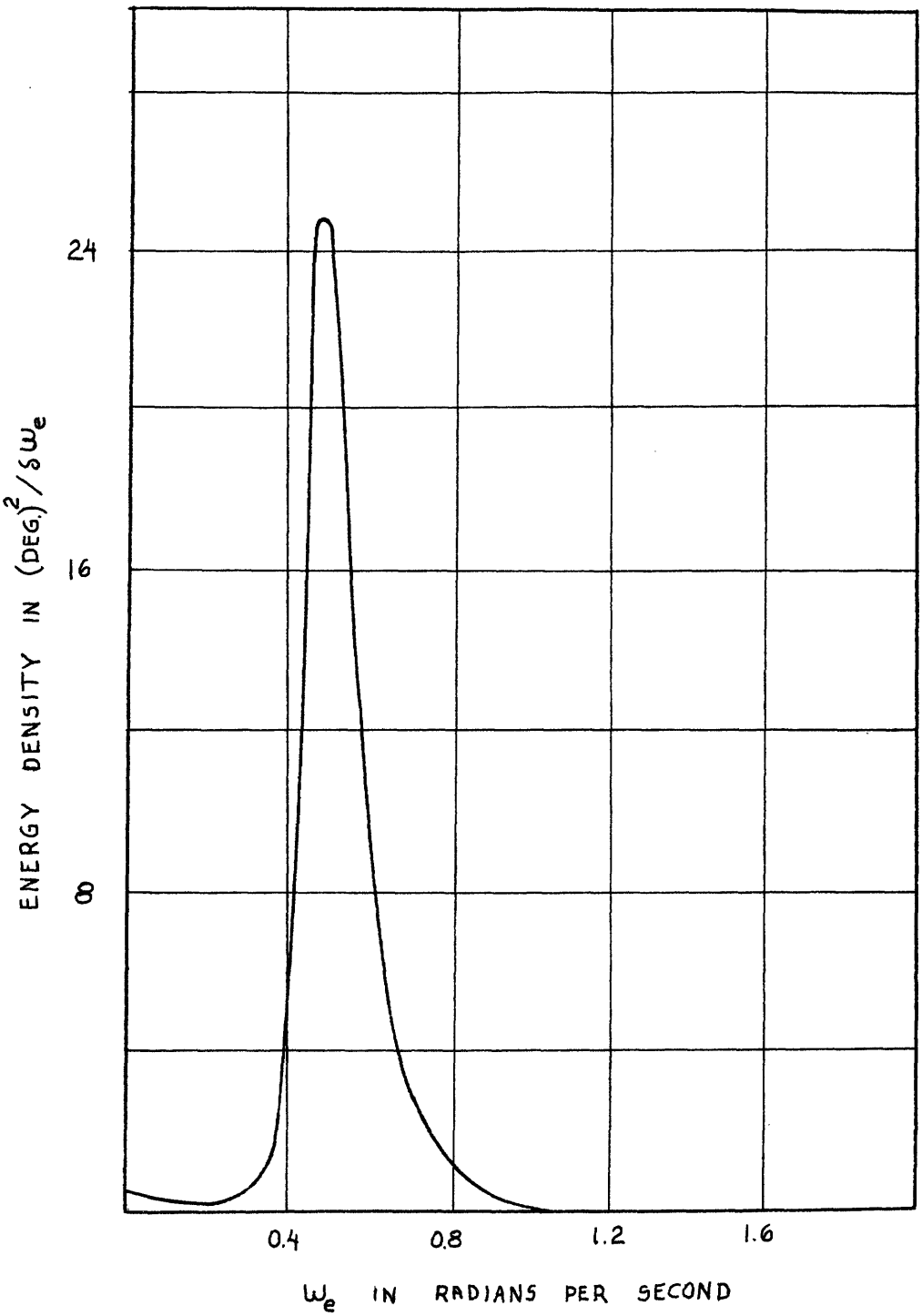

Figure 6.1 Energy Spectrum for Roll Amplitude

roughly $2\pi/0.5$ or 12.5 seconds, any reasonably accurate integration technique for a continuous function would have to use integration steps on the order of several hundredths, or at most, tenths of seconds. Use of such small integration steps would result in simulation times which would be comparable to the real time being simulated. Since reset intervals are on the order of several hours, such a simulation would be too costly. In an actual system, the integration computations would be performed on a Digital Differential Analyzer, which is much better suited to the generation of the weighting functions.

A scheme which overcomes this difficulty is the following:

If the rolling and pitching motion is described by a train of rectangular pulses, the elements of the direction cosine matrix will change their values in discrete steps, while remaining constant between these steps. Thus, the time consuming iterative integration process is not required. Instead, evaluation of the weighting functions now reduces to much faster summation operations.

Use of a rectangular wave process to simulate vehicle motion, which is actually sinusoidal in nature, can be justified if the process has a spectrum similar to that shown in Figure 6.1. From a statistical standpoint, the discontinuous motion will have the same effect on the weighting functions as would the continuous motion.

Thus the problem remains of finding a rectangular wave process which possesses a spectrum similar to that shown in Figure 6.1.

Consider a periodic wave of rectangular pulses whose amplitude reverses sign every $T/2$ seconds and is normally distributed with mean M and standard deviation σ. Examples of this process are shown in Figures 6.2 and 6.3.

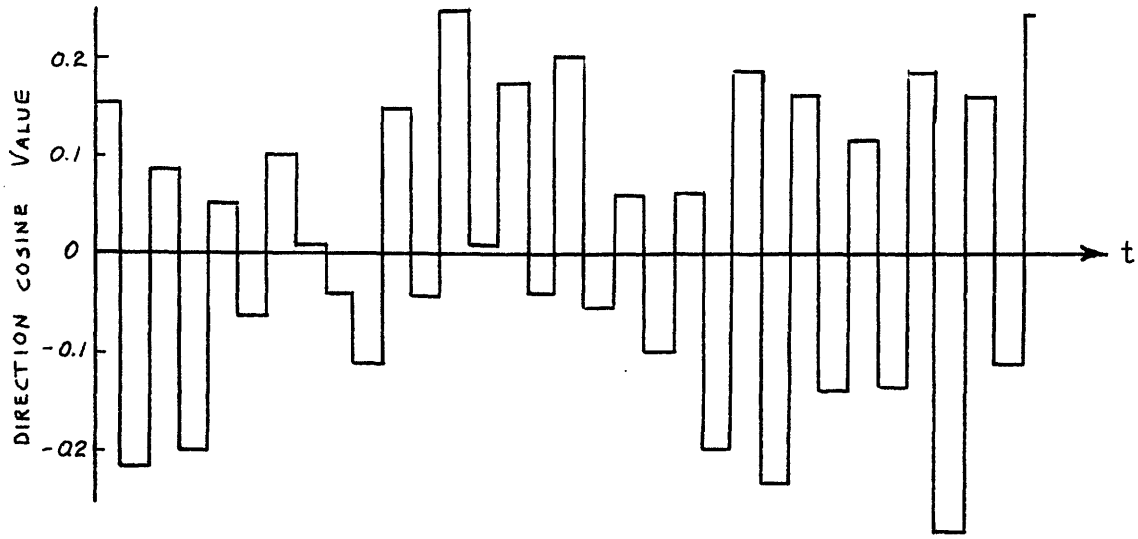

Figure 6.2 Roll Motion Model

($M = 6.735^{\circ}$, $\sigma = 4.76^{\circ}$)

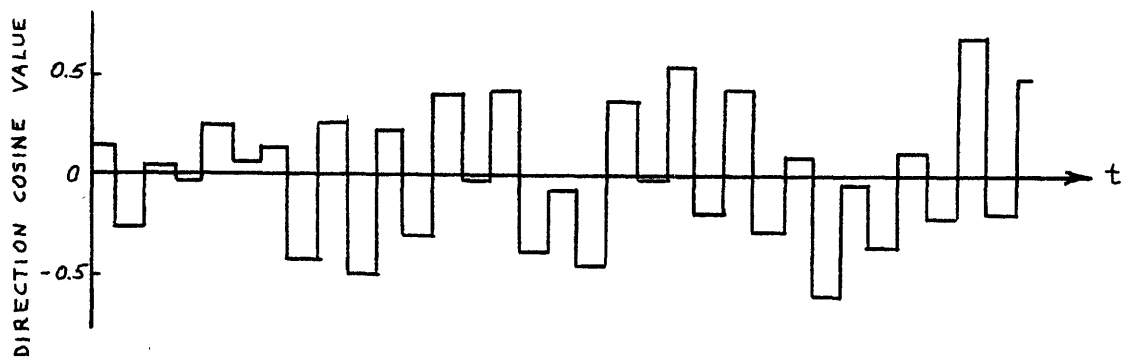

Figure 6.3 Roll Motion Model

($M = 15^{\circ}$, $\sigma = 10.5^{\circ}$)

The probability density function of the amplitude, x, is given by,

$$f(x) = \frac{1}{\sqrt{2\pi}\sigma} e^{\frac{-(x-M)^2}{2\sigma^2}} \tag{6-1}$$

As derived in Appendix C, the autocorrelation function corresponding to this process is shown in Figure 6.4. This function can be separated into a periodic component (Figure 6.5) and a random component (Figure 6.6).

The power spectrum for the periodic component is

$$\Phi_{pp}(n\omega_o) = \left(M^2 \left(\frac{\sin\left(\frac{n\pi}{2}\right)}{\frac{n\pi}{2}} \right)^2 \right) \qquad n = \pm 1, \pm 3, \pm 5, \cdots \tag{6-2}$$

where $\omega_o = \frac{2\pi}{T}$.

The power density spectrum of the random component is,

$$\Phi_{rr}(\omega) = \frac{\sigma^2}{2\omega_o} \left(\frac{\sin\left(\frac{\omega T}{4}\right)}{\frac{\omega T}{4}} \right)^2 \tag{6-3}$$

Derivations of these expressions can be found in Appendix C. The two spectra are plotted in Figures 6.7 and 6.8.

It is intended that rectangular waves of this type be used to describe the values of the direction cosines which will be oscillating about zero. The other elements of the matrix can then be determined using the orthogonality constraints placed on the direction cosine matrix.

Comparison of Figure 6.1 with Figures 6.7 and 6.8 shows that there seems to be little similarity between the experimental and rectangular wave spectra. Hence one would think that the proposed rectangular wave process will not realistically describe vehicle motion. However, a closer examination of the problem at hand will show that this process is indeed adequate for the purposes of this study.

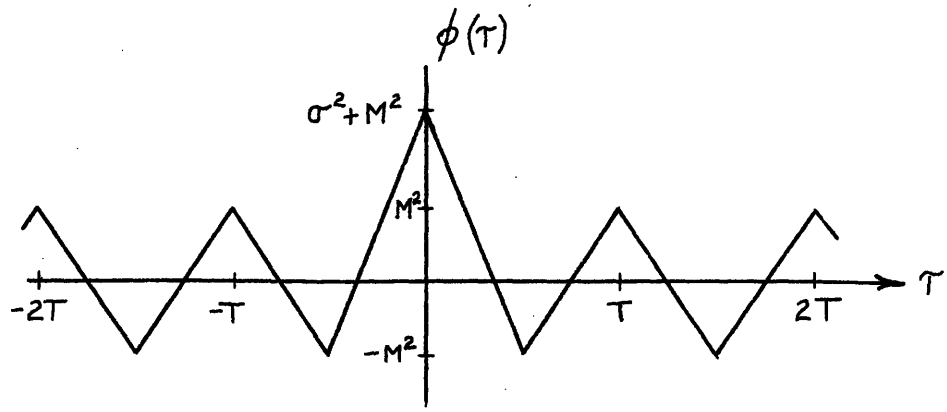

Figure 6.4 Autocorrelation Function of Model

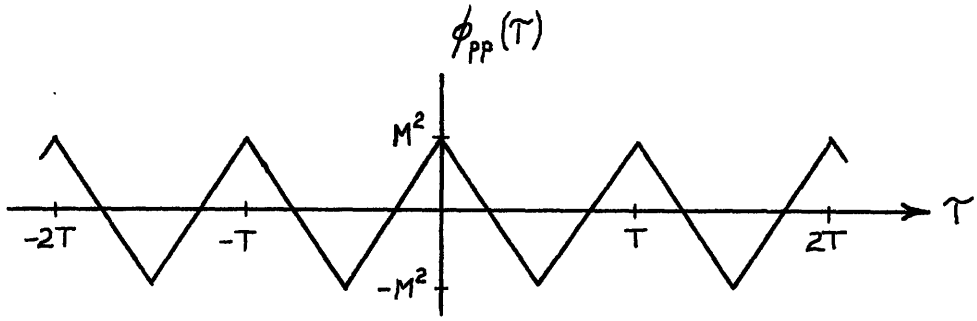

Figure 6.5 Periodic Component of Autocorrelation Function

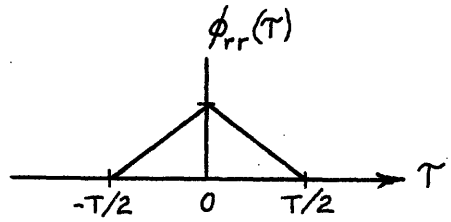

Figure 6.6 Random Component of Autocorrelation Function

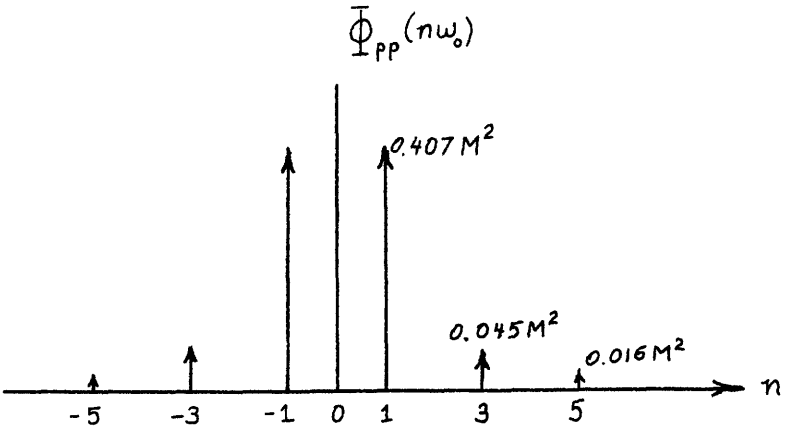

Figure 6.7 Power Spectrum of Periodic Component

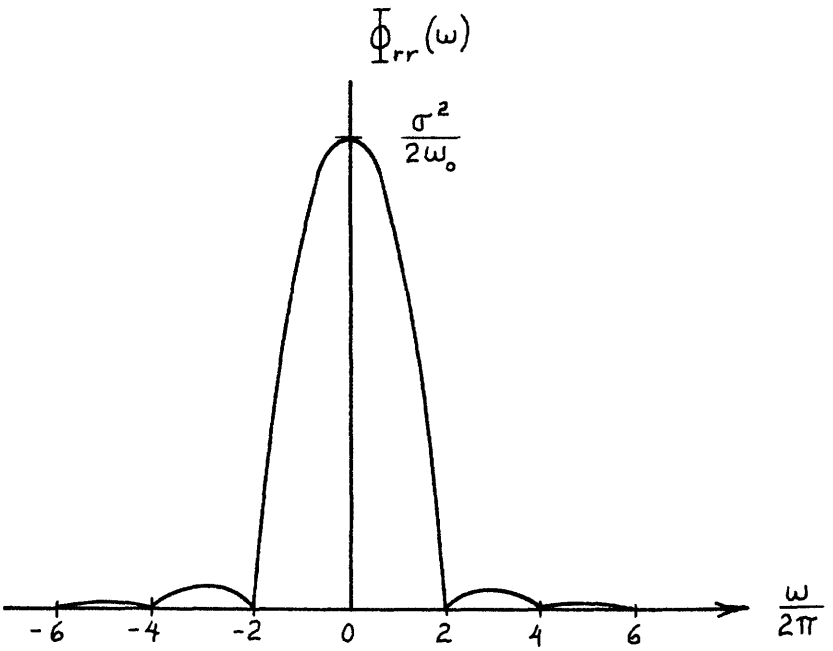

Figure 6.8 Power Density Spectrum of Random Component

Vehicle motion can be viewed as being composed of a low frequency component and a high frequency component. The low frequency changes in the direction cosine matrix correspond to changes in the vehicle's heading. The high frequency modulation of the direction cosines is caused by the rolling and pitching motion. Thus, the direction cosines between the x and y axes of the vehicle and the x and y axes of the geographic system will, in general, have both low and high frequency components. The direction cosines C_z^x, C_z^y, C_x^z, and C_y^z will be composed of only high frequencies since they are proportional to the roll and pitch angles only, and not ship's heading.

We have previously seen that each weighting function used in determining the unknown drift constants is computed as a solution of a convolution integral. The weighting function can thus be physically interpreted as being the output signal of an electrical circuit in response to some input signal. The electrical circuits were found, in Chapter 5, to be simple harmonic oscillators, or L-C filters, with earth's rate as their natural frequency. The input signals to these filters are the analogs of the drift forcing functions, expressed as functions of the direction cosines.

In the present study, we are primarily interested in the magnitude of weighting functions generated by the direction cosines which only contain high frequency components. From the standpoint of the electrical analog, we are essentially trying to determine the output of a filter tuned to 7.3×10^{-5} radians per second when excited by high frequency signals. Since almost all of the input signals, as can be seen in Figure 6.1, are of frequencies much higher than 7.3×10^{-5} radians per second, it can safely be assumed that the majority of these signals is concentrated at one high frequency. The discrete spectrum of Figure 6.7 will thus adequately describe the high frequency inputs. The power density spectrum of Figure 6.8 will then provide the low frequency input power. The justification for using the rectangular wave process hinges on the fact that we are basically interested in the magnitude of the weighting function.

6.3 The Weighting Function

When the direction cosines are described by rectangular pulses, solution of the convolution integral reduces to a simple summation operation.

As an example, consider a typical weighting function of the form,

$$F(t) = \cos\Omega t \int_0^t \cos\Omega\tau\, C_y^x\, d\tau + \sin\Omega t \int_0^t \sin\Omega\tau\, C_y^x\, d\tau \tag{6-4}$$

Since C_y^x changes its value every $T/2$ seconds and remains constant within this interval, (6-4) can be written as,

$$F(t_n) = \cos\Omega t_n \sum_{i=0}^{n-1} C_y^x \int_{t_i}^{t_{i+1}} \cos\Omega\tau\, d\tau + \sin\Omega t_n \sum_{i=0}^{n-1} C_y^x \int_{t_i}^{t_{i+1}} \sin\Omega\tau\, d\tau \tag{6-5}$$

where $t_n = nT/2$ and $t_{i+1} - t_i = T/2$.

But

$$\int_{t_i}^{t_{i+1}} \cos\Omega\tau\, d\tau = \frac{1}{\Omega}\left(\sin\Omega t_{i+1} - \sin\Omega t_i\right) = \frac{2}{\Omega}\left(\cos\frac{\Omega}{2}(t_{i+1}+t_i)\,\sin\frac{\Omega}{2}(t_{i+1}-t_i)\right) \tag{6-6}$$

Approximating $(t_{i+1} + t_i)/2$ by t_i,

$$\int_{t_i}^{t_{i+1}} \cos\Omega\tau\, d\tau = \frac{2}{\Omega}\cos\Omega t_i \sin\frac{\Omega T}{4} \tag{6-7}$$

Similarly,

$$\int_{t_i}^{t_{i+1}} \sin\Omega\tau\, d\tau = \frac{2}{\Omega} \sin\Omega t_i \sin\frac{\Omega T}{4} \tag{6-8}$$

Substituting (6-7) and (6-8) into (6-5),

$$F(t_n) = K\left[\cos\Omega t_n \sum_{i=0}^{n-1} C_i^x \cos\Omega t_i + \sin\Omega t_n \sum_{i=0}^{n-1} C_i^x \sin\Omega t_i\right] \tag{6-9}$$

where $K = 2 \sin\frac{\Omega T}{4} / \Omega$.

In a simulation, the digital computer would solve equation (6-9) by continuously performing the indicated summation operations as time is incremented. Then, when a fix is taken, the whole weighting function is evaluated and stored for later use in computing the unknown drift constants.

6.4 Simulations

At the outset of the simulation study, it was decided to assume only constant drifts. Inclusion of the mass unbalance drift components would result in a significant increase in computer time, without appreciably contributing any new information. In all runs, an initial drift of 1 degree per hour was used for all three gyros. For the sake of simplicity, it was also decided that the vehicle have no translational motion, and maintain a constant zero heading. The placing of a constraint on heading is not germane to the problem since heading changes will be of very low frequency and will not affect the high frequency motion which is presently of interest. Also, if the vehicle is oriented with its roll axis pointing north, the vehicle's coordinate system will remain roughly aligned with its geographic axes, as in the case of a gimbaled system. Thus, a comparison with error curves from previous

studies on gimbaled systems can be made to provide a check on the reset equations being used in the computer program. In order that several reset intervals could be simulated in a reasonable amount of computer time, the further simplifying assumption of simulating only roll motion was made. This assumption is not serious since simulating both pitch and roll motion would essentially mean only increasing the number of weighting functions that must be computed. The character of the high frequency direction cosines, and their effect on the weighting functions will still be realistic.

When only roll motion is present, the geometry of the coordinate systems dictates that C_z^x and C_x^z be zero. The direction cosines, C_y^z and C_z^y, will therefore be the only oscillating terms that will be neglected in effecting the simplified reset computations. A block diagram of the simulation program is presented in Appendix D.

The first set of reset simulations were performed under the condition that only latitude and longtitude fixes were available. The mean value of the simulated roll motion, that is, the mean value of the amplitude of the rectangular pulses, corresponded to the most severe experimental rolling data, which occured when the vehicle was proceeding on the surface of a state 5 sea at 15 knots. In reference 22, this value is given as 6.735 degrees. The standard deviation of the amplitude was chosen to correspond to .707 times the mean, or about 4.76°.

In the first run, no reset was made. The errors generated over a 28 hour period are shown in Figure 6.9. Since the ship's heading was kept at zero, the error curves showed close similarity with errors generated in a gimbaled system. The latitude and azimuth errors are 90 degrees out of phase, and hence, if plotted on the $\delta\lambda$, $\gamma \cos \lambda$ phase-plane, would result in a circle diagram.

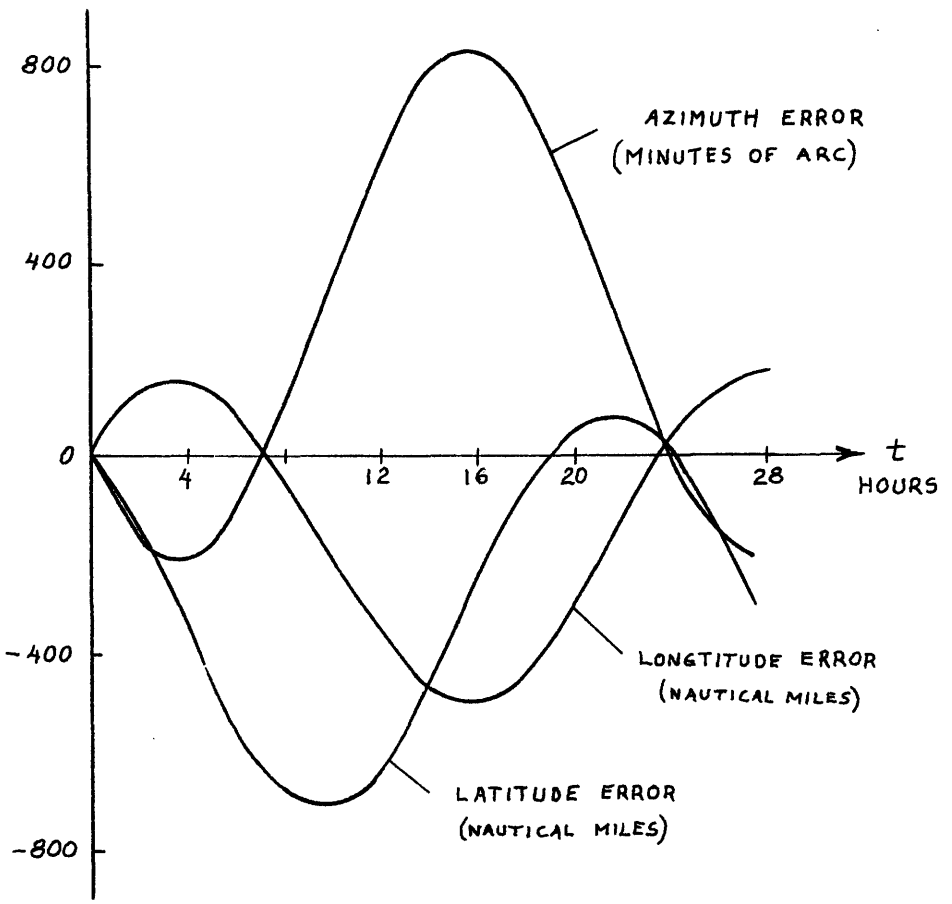

Figure 6.9 System Errors Without Resets

(1°/hr. drift in all gyros)

In the second run, a fix interval of 3.5 hours was used. Since only latitude and longtitude could be fixed at the end of each fix interval, two fix intervals were required to make a reset. Actually two fixes on latitude and one longtitude fix, taken at the end of the second fix interval, were used to determine the three drift constants. In this second run, no simplifications were made in computing the weighting functions. This run thus served as a check on programming errors. Due to round-off error in the digital computer, the computed drifts were not exactly $1°$/hour. The error was very small (approximately one part in 10^8) however, and could be neglected.

The resets in the third simulation were made using the simplified weighting functions. The simplified weighting functions were computed in the same way as was done in the previous run, except that terms involving C_y^z and C_z^y were neglected. Figures 6.10, 6.11, and 6.12 show the time histories of the latitude, longtitude, and azimuth errors, respectively. The azimuth error curve is not entirely correct after the first reset. A bias value, corresponding to the error of the computed azimuth correction, should be added to the plotted values. The bias is approximately 3.58 minutes of arc. The latitude and longtitude curves are correct since perfect fixes have been assumed here.

In order to judge the effectiveness of the simplified resets, errors in the computed drifts, as compared with their true values, were computed. These errors are presented in Table 6.1 as percentages. The last column of the table shows the errors in the computed azimuth corrections.

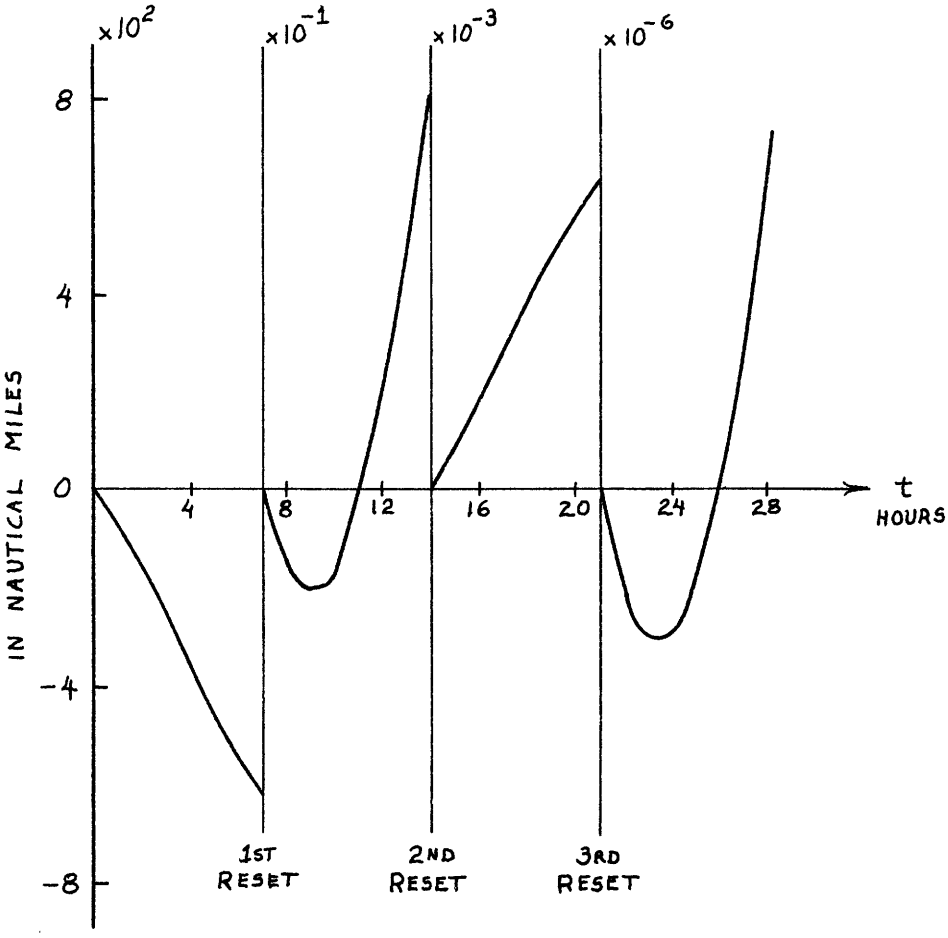

Figure 6.10 Latitude Error With Resets

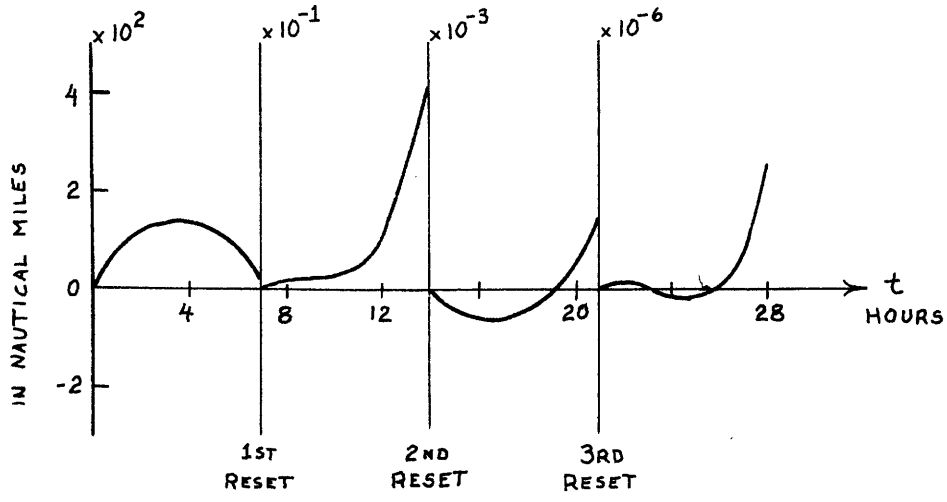

Figure 6.11 Longtitude Error With Resets

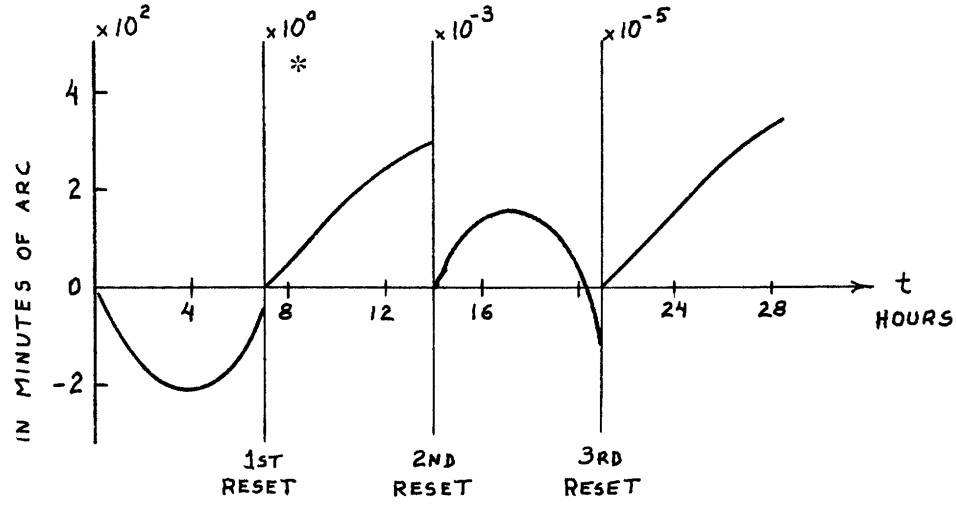

Figure 6.12 Azimuth Error With Resets

* A bias error of 3.58 minutes of arc has not been included

TABLE 6.1

SIMPLIFIED RESET ERRORS FOR
LATITUDE AND LONGTITUDE FIXES
($M = 6.735°$, $\sigma = 4.76°$)

	X-Gyro Drift (%)	Y-Gyro Drift (%)	Z-Gyro Drift(%)	AZ(%)
1st Reset	2.83	.355	3.16	11.3
2nd Reset	.011	.344	.061	.045
3rd Reset	8.8	.36	1.66	3.87
4th Reset	.244	2.7	.233	.243

The next series of simulations involved resets using latitude, longtitude, and azimuth fixes. Because the errors of the previous run were relatively small, the mean and standard deviation of the roll angles was increased to 15° and 10.5°, respectively.

Since three quantities were now being fixed, a reset could be performed at the end of each 3.5 hour fix interval. In the first run of this series, no reset was performed. The error curves were almost identical to those shown in Figure 6.9, which points out the small effect high frequencies have on the reset computations. The second run was again used as a check on reset equation programming errors. Finally, in the third simulation, the simplified weighting functions were used to compute the drifts. The errors for the simplified reset are shown in Table 6.2

TABLE 6.2

SIMPLIFIED RESET ERRORS FOR
LATITUDE, LONGTITUDE AND AZIMUTH FIXES
($M = 15°$, $\sigma = 10.5°$)

	X-Gyro Drift (%)	Y-Gyro Drift (%)	Z-Gyro Drift (%)
1st Reset	.421	.341	.124
2nd Reset	.726	.184	.581
3rd Reset	.005	.176	.053

Comparison of the errors of Tables 6.1 and 6.2 shows that even though more violent rolling was simulated, the second set of errors are noticeably smaller and more consistant. This is due to the fact that two fixes on latitude were used in computing the first set, whereas the more accurate resets were based on fixes of three different quantities. This effect was mentioned earlier in this thesis when the independence of fixes was discussed. The larger errors resulted because there was some, although very little, linear dependence between the two latitude fixes. An indication of this dependence can be seen in Figure 6.9. In the first reset interval, ($0 < T < 7$), and in the third reset interval ($14 < T < 21$), the latitude error curve is roughly linear. Thus the first and third resets show relatively large errors in Table 6.1. In the second and fourth reset intervals, however, the latitude error curve does not show much linearity. Hence, in Table 6.1, the errors for these resets are relatively small. Although such linear dependency would be rare in the case of a vehicle which changes its heading, the above case vividly emphasizes the care that must be taken when obtaining fixes.

6.5 Discussion of the Simulation Results

The simulations have shown that neglecting the cross coupling direction cosines which contain only high frequency components, in the generation of the weighting functions will result in computed drift errors on the order of a few percent, at most. Since the submarine, will normally be submerged, where rolling and pitching motion will be small, the resulting errors should be even smaller. Moreover, since the reset solution is already based on the assumption of constant drift, the actual variations of drift would influence the effectiveness of the reset solution as much as, if not more than, the simplification under study.

If mass unbalance drifts are also being solved for, similar simplifications can be made. Because mass unbalance weighting functions involve products of direction cosines, care must be used in determining which terms may be neglected.

CHAPTER 7

SUMMARY, CONCLUSIONS, AND RECOMMENDATIONS

7.1 Summary

Errors in an inertial navigation system produced by gyro drift tend to accumulate with time. The determination and subsequent removal of gyro drift is therefore mandatory if the system is to remain within operational specifications over extended periods of time. The purpose of this thesis was to devise a means of determining gyro drift in a modified-strapped-down system using position and/or heading fix information.

The general method of gyro drift determination developed in this thesis is continuously to compute system errors which would be generated by unit, or normalized, drifts. The actual values of the errors are intermittently determined with the externally-obtained fix information. When a certain minimum number of fixes has been taken, the gyro drifts can be evaluated. A reset is then made in which 1) the computed gyro drift is removed and 2) the system output errors are corrected. Corrections to system outputs which have not been measured directly by fixes may be determined by evaluating the corresponding normalized errors with the computed drift values. Besides the equipment required to make the fix measurements, the only addition to the navigation system to instrument resets is a computer. The size of this computer depends on the drift model being used.

As a realistic example, application of this reset method has been made to a strapped-down inertial navigation system for a submarine. In this study, a drift model consisting of superimposed constant drift and dynamic mass-unbalance drift was used. The error equations for latitude, longtitude, and azimuth, as can be seen in Appendix B, are fairly lengthy because of the oscillatory nature of the basic navigation equations.

The error equations can be simplified to some extent by assuming that submarine motion is restricted to a plane. The simulation study has shown that neglecting the high-frequency motion of rolling and pitching will result in computed drift errors of the order of a few percent. The feasibility of incorporating this simplification will, of course, depend on the system's performance specifications.

7.2 Conclusions

The theoretical feasibility of a method for determining gyro drift and output error corrections for a modified-strapped-down inertial navigation system has been demonstrated. Although no quantitative conclusions concerning the effectiveness of the method can be drawn from this thesis, the reset method is sound under the following assumptions;

1) gyro drift in a strapped-down environment is realistically described by a drift model consisting of superimposed constant drift and dynamic mass unbalance drift
2) fix measurements are made without error
3) reset computations are performed without error

7.3 Recommendations

As a logical continuation of this investigation it is recommended that:

1) extensive experiments be performed to determine a realistic drift model for gyros in the strapped-down environment
2) an error analysis be made to determine the sensitivity of the reset method to fix errors and computational errors.
3) the actual mechanization of the required reset computations be investigated. A Digital Differential Analyzer appears to be best suited to performing the real-time multiplication and integration operations.

APPENDIX A

DERIVATION OF THE ERROR MATRIX FOR A GIMBALED SYSTEM

The specific force measured by the accelerometers is, in vector form,

$$\bar{f} = -\ddot{\bar{R}} - 2\bar{W}\times\dot{\bar{R}} - \dot{\bar{W}}\times\bar{R} - \bar{W}\times(\bar{W}\times\bar{R}) + \bar{G} \tag{A-1}$$

where $\bar{G}$ is the gravitation vector, $\bar{R}$ is the position vector measured from the origin of the coordinate frame, and $\bar{W}$ is the angular velocity of the coordinate frame.

Let t refer to the vehicle's local geographic coordinate system. The z-axis of this orthogonal system is normal to the reference ellipsoid, the x-axis points north, and the y-axis points east, completing the right-handed set. It can be shown[13] that the x and y components of the specific force, derived from (A-1), can be expressed fairly accurately as,

$$\begin{aligned} f_{tx} &= -2W_N\dot{R} - \dot{W}_N R - 2\Omega W_E R\sin\lambda - W_E^2 R\tan\lambda \\ f_{ty} &= -2\Omega\dot{R}\cos\lambda - 2W_E\dot{R} - \dot{W}_E R + 2\Omega W_N R\sin\lambda \\ &\quad + W_E W_N R\tan\lambda \end{aligned} \tag{A-2}$$

where Ω = earth's rotation rate

W_N = rate of change of geographic latitude

W_E = rate of change of longtitude

λ = geographic latitude

$c = (a^2-b^2)/2ab$, where a and b are the semi-major and semi-minor axes of the reference ellipsoid, respectively

Since, for a submarine, $\dot{R}$ is small, (A-2) can be rewritten as,

$$\dot{W}_E = -\frac{1}{R}\left(f_{iy} - W_E W_N R\,TAN\lambda - 2\Omega W_N R\,SIN\lambda\right)$$
$$\dot{W}_N = -\frac{1}{R}\left(f_{ix} + W_E^2 R\,TAN\lambda + 2\Omega W_E R\,SIN\lambda\right) \qquad \text{(A-3)}$$

If the subscript, C, denotes computed values,

$$\dot{W}_{EC} = -\frac{1}{R}\left(f_{iy} - W_{EC} W_{NC} R\,TAN\lambda_c - 2\Omega W_{NC} R\,SIN\lambda_c\right)$$
$$\dot{W}_{NC} = -\frac{1}{R}\left(f_{ix} + W_{EC}^2 R\,TAN\lambda_c + 2\Omega W_{EC} R\,SIN\lambda_c\right) \qquad \text{(A-4)}$$

The angular rates of the controlled member are[13]

$$W_{ix} = \Omega\cos\lambda_c + W_{EC} + U_x$$
$$W_{iy} = -W_{NC} + U_y$$
$$W_{iz} = -\Omega\,SIN\lambda_c - W_{EC}\,TAN\lambda_c + U_z \qquad \text{(A-5)}$$

where U_x, U_y, and U_z are the gyro drift rates.

The submarine is inherently a slow moving vehicle. Hence W_N and W_E will be small compared to the earth's rotation. If the submarine is assumed to be stationary on the surface of the earth, the gravity, g, will be the only specific force acting on the vehicle and,

$$f_{tx} = f_{ty} = 0$$
$$f_{tz} = g \qquad \text{(A-6)}$$

The specific force measured in the indicated system is

$$\bar{f}_i = C_i^t \bar{f}_t \qquad \text{(A-7)}$$

C_i^t is the transformation matrix between the t and i systems. Since the two systems are almost coincident, it can be expressed as,

$$C_i^t = \begin{bmatrix} 1 & \gamma & -\beta \\ -\gamma & 1 & \alpha \\ \beta & -\alpha & 1 \end{bmatrix} \tag{A-8}$$

α, β and γ are the components in the i system of a virtual vector rotation that would carry the t system into coincidence with the i system. α and β are called the vertical errors and γ is called the azimuth error.

From (A-6), (A-7) and (A-8),

$$\begin{aligned} f_{ix} &= -\beta g \\ f_{iy} &= \alpha g \end{aligned} \tag{A-9}$$

Let the errors quantities be defined by

$$\begin{aligned} \delta\dot{W}_E &= \dot{W}_{EC} - \dot{W}_E \\ \delta\dot{W}_N &= \dot{W}_{NC} - \dot{W}_N \\ \delta W_E &= W_{EC} - W_E \\ \delta W_N &= W_{NC} - W_N \\ \delta\lambda &= \lambda_c - \lambda \end{aligned} \tag{A-10}$$

With the imposed condition of a stationary vehicle,

$$\dot{W}_E = \dot{W}_N = W_E = W_N = 0 \tag{A-11}$$

the error equations

$$\begin{aligned} \delta\dot{W}_N &= -\delta W_E\, 2\Omega \sin\lambda + \beta(g/R) \\ \delta\dot{W}_E &= \delta W_N\, 2\Omega \sin\lambda - \alpha(g/R) \end{aligned} \tag{A-12}$$

are obtained if second order terms are neglected. To these may be added the definition

$$\begin{aligned} W_{NC} - W_N &= \frac{d}{dt}(\lambda_c - \lambda) \\ \delta W_N &= \delta\dot{\lambda} \end{aligned} \tag{A-13}$$

It is shown in Reference (13) that

$$\dot{C}_t^i = C_t^i W_i - W_t C_t^i \tag{A-14}$$

where C_t^i is the transpose of C_i^t,

W_i is computed angular velocity of the indicated frame

W_t is the angular velocity of the actual geographic frame and is of the form,

$$W_t = \begin{bmatrix} 0 & -W_{tz} & W_{ty} \\ W_{tz} & 0 & -W_{tx} \\ -W_{ty} & W_{tx} & 0 \end{bmatrix} \tag{A-15}$$

Premultiplying $\dot{C}_t^i$ by C_i^t,

$$C_i^t \dot{C}_t^i = W_i - C_i^t W_t C_t^i \tag{A-16}$$

C_i^t can be written as

$$C_i^t = I + A \tag{A-17}$$

where I is the unit matrix and

$$A = \begin{bmatrix} 0 & \gamma & -\beta \\ -\gamma & 0 & \alpha \\ \beta & -\alpha & 0 \end{bmatrix} \tag{A-18}$$

Therefore,

$$\dot{C}_t^i = -\dot{A} \tag{A-19}$$

and $C_i^t \dot{C}_t^i$ can be approximated by

$$C_i^t \dot{C}_t^i = (I+A)(-\dot{A}) \approx -\dot{A} \tag{A-20}$$

if second order terms are neglected.

Equation (A-16) then becomes

$$-\dot{A} = W_i - C_i^t W_t C_t^i \tag{A-21}$$

Using the similarity transformation of almost coicident Cartesian coordinates, (A-19) can be written in vector form as

$$-\dot{\overline{A}} = \overline{W_i} - C_i^t \overline{W_t} \tag{A-22}$$

The angular velocity vector of a stationary geographic system is, [13]

$$\begin{aligned} W_{tx} &= \Omega \cos\lambda \\ W_{ty} &= 0 \\ W_{tz} &= -\Omega \sin\lambda \end{aligned} \tag{A-23}$$

Using (A-5), (A-8), (A-20) and (A-21),

$$\begin{aligned} \dot{\alpha} &= -\Omega\,\delta\lambda \sin\lambda + \delta W_E - \beta\Omega \sin\lambda + u_x \\ \dot{\beta} &= -\delta W_N + \alpha\Omega \sin\lambda + \gamma\Omega\cos\lambda + u_y \\ \dot{\gamma} &= -\delta\lambda\,\Omega\cos\lambda - \delta W_E \tan\lambda - \beta\Omega\cos\lambda + u_z \end{aligned} \tag{A-24}$$

Equations (A-12), (A-13) and (A-24) are presented in matrix form as (A-25).

$$
\begin{bmatrix} \dot{\delta W}_N \\ \dot{\delta W}_E \\ \dot{\delta\lambda} \\ \dot{\alpha} \\ \dot{\beta} \\ \dot{\gamma} \end{bmatrix}
=
\left[\begin{array}{c|c|c|c|c|c}
0 & -2\Omega\sin\lambda & 0 & 0 & g/R & 0 \\
\hline
2\Omega\sin\lambda & 0 & 0 & -g/R & 0 & 0 \\
\hline
1 & 0 & 0 & 0 & 0 & 0 \\
\hline
0 & 1 & -\Omega\sin\lambda & 0 & -\Omega\sin\lambda & 0 \\
\hline
-1 & 0 & 0 & \Omega\sin\lambda & 0 & \Omega\cos\lambda \\
\hline
0 & -\tan\lambda & -\Omega\cos\lambda & 0 & -\Omega\cos\lambda & 0
\end{array}\right]
\begin{bmatrix} \delta W_N \\ \delta W_E \\ \delta\lambda \\ \alpha \\ \beta \\ \gamma \end{bmatrix}
+
\begin{bmatrix} 0 \\ 0 \\ 0 \\ u_x \\ u_y \\ u_z \end{bmatrix}
$$

(A-25)

APPENDIX B

STRAPPED-DOWN SYSTEM ERROR EQUATIONS

Expressions for the latitude, longtitude and azimuth errors are presented in this appendix. The latitude error, $\delta\lambda$, is derived for constant and mass unbalance drifts. The longtitude error, $\delta\ell$, and the azimuth error, γ, equations are for constant drifts only.

$$
\begin{aligned}
\delta\lambda(t) = \; & -u_{kx}\Bigg[\cos\Omega t\int_0^t\Big[\cos\Omega\tau\, C_y^x - \sin\Omega\tau\left(\sin\lambda\, C_x^x + \cos\lambda\, C_z^x\right)\Big]d\tau \\
& \quad + \sin\Omega t\int_0^t\Big[\sin\Omega\tau\, C_y^x + \cos\Omega\tau\left(\sin\lambda\, C_x^x + \cos\lambda\, C_z^x\right)\Big]d\tau\Bigg] \\
& -u_{ky}\Bigg[\cos\Omega t\int_0^t\Big[\cos\Omega\tau\, C_y^y - \sin\Omega\tau\left(\sin\lambda\, C_x^y + \cos\lambda\, C_z^y\right)\Big]d\tau \\
& \quad + \sin\Omega t\int_0^t\Big[\sin\Omega\tau\, C_y^y + \cos\Omega\tau\left(\sin\lambda\, C_x^y + \cos\lambda\, C_z^y\right)\Big]d\tau\Bigg] \\
& -u_{kz}\Bigg[\cos\Omega t\int_0^t\Big[\cos\Omega\tau\, C_y^z - \sin\Omega\tau\left(\sin\lambda\, C_x^z + \cos\lambda\, C_z^z\right)\Big]d\tau \\
& \quad + \sin\Omega t\int_0^t\Big[\sin\Omega\tau\, C_y^z + \cos\Omega\tau\left(\sin\lambda\, C_x^z + \cos\lambda\, C_z^z\right)\Big]d\tau\Bigg] \\
& -u_{SAx}\Bigg[\cos\Omega t\int_0^t\Big[\cos\Omega\tau\, C_y^x C_z^x - \sin\Omega\tau\, C_z^x\left(\sin\lambda\, C_x^x + \cos\lambda\, C_z^x\right)\Big]d\tau \\
& \quad + \sin\Omega t\int_0^t\Big[\sin\Omega\tau\, C_y^x C_z^x + \cos\Omega\tau\, C_z^x\left(\sin\lambda\, C_x^x + \cos\lambda\, C_z^x\right)\Big]d\tau\Bigg]\frac{g_o}{H} \\
& -u_{SAy}\Bigg[\cos\Omega t\int_0^t\Big[\cos\Omega\tau\, C_y^y C_z^y - \sin\Omega\tau\, C_z^y\left(\sin\lambda\, C_x^y + \cos\lambda\, C_z^y\right)\Big]d\tau \\
& \quad + \sin\Omega t\int_0^t\Big[\sin\Omega\tau\, C_y^y C_z^y + \cos\Omega\tau\, C_z^y\left(\sin\lambda\, C_x^y + \cos\lambda\, C_z^y\right)\Big]d\tau\Bigg]\frac{g_o}{H} \\
& -u_{SAz}\Bigg[\cos\Omega t\int_0^t\Big[\cos\Omega\tau\, C_y^z C_z^z - \sin\Omega\tau\, C_z^z\left(\sin\lambda\, C_x^z + \cos\lambda\, C_z^z\right)\Big]d\tau \\
& \quad + \sin\Omega t\int_0^t\Big[\sin\Omega\tau\, C_y^z C_z^z + \cos\Omega\tau\, C_z^z\left(\sin\lambda\, C_x^z + \cos\lambda\, C_z^z\right)\Big]d\tau\Bigg]\frac{g_o}{H}
\end{aligned}
$$

$$
\begin{aligned}
-U_{IA_x}\Bigg[&\cos\Omega t\int_0^t\left(\cos\Omega\tau\,C_y^x-\sin\Omega\tau\left(\sin\lambda\,C_x^3+\cos\lambda\,C_3^x\right)\right)\left(-C_3^y\cos\theta_x-C_3^3\sin\theta_x\right)\Big]\,d\tau\\
&+\sin\Omega t\int_0^t\Big[\sin\Omega\tau\,C_y^x+\cos\Omega\tau\left(\sin\lambda\,C_x^3+\cos\lambda\,C_3^x\right)\Big)\left(-C_3^y\cos\theta_x-C_3^3\sin\theta_x\right)\Big]\,d\tau\Bigg]\frac{g_0}{H}\\
-U_{IA_y}\Bigg[&\cos\Omega t\int_0^t\Big[\cos\Omega\tau\,C_y^y-\sin\Omega\tau\left(\sin\lambda\,C_x^y+\cos\lambda\,C_3^y\right)\Big)\left(C_3^x\cos\theta_y-C_3^3\sin\theta_y\right)\Big]\,d\tau\\
&+\sin\Omega t\int_0^t\Big[\sin\Omega\tau\,C_y^y+\cos\Omega\tau\left(\sin\lambda\,C_x^y+\cos\lambda\,C_3^y\right)\Big)\left(C_3^x\cos\theta_y-C_3^3\sin\theta_y\right)\Big]\,d\tau\Bigg]\frac{g_0}{H}\\
-U_{IA_3}\Bigg[&\cos\Omega t\int_0^t\Big[\cos\Omega\tau\,C_y^3-\sin\Omega\tau\left(\sin\lambda\,C_x^3+\cos\lambda\,C_3^3\right)\Big)\left(C_3^x\cos\theta_3+C_3^y\sin\theta_3\right)\Big]\,d\tau\\
&+\sin\Omega t\int_0^t\Big[\sin\Omega\tau\,C_y^3+\cos\Omega\tau\left(\sin\lambda\,C_x^3+\cos\lambda\,C_3^3\right)\Big)\left(C_3^x\cos\theta_3+C_3^y\sin\theta_3\right)\Big]\,d\tau\Bigg]\frac{g_0}{H}
\end{aligned}
$$

$$
\begin{aligned}
\delta\ell(t) = u_{kx} \Bigg[& \cos\lambda \int_0^t C_x^x \, d\tau - \sin\lambda \int_0^t C_z^x \, d\tau \\
& + \cos\Omega t \int_0^t \left[\cos\Omega\tau \sin\lambda \tan\lambda \, C_x^x + \sin\Omega\tau \tan\lambda \, C_y^x + \cos\Omega\tau \sin\lambda C_z^x \right] d\tau \\
& + \sin\Omega t \int_0^t \left[\sin\Omega\tau \sin\lambda \tan\lambda \, C_x^x - \cos\Omega\tau \tan\lambda \, C_y^x + \sin\Omega\tau \sin\lambda C_z^x \right] d\tau \Bigg] \\
+ u_{ky} \Bigg[& \cos\lambda \int_0^t C_x^y \, d\tau - \sin\lambda \int_0^t C_z^y \, d\tau \\
& + \cos\Omega t \int_0^t \left[\cos\Omega\tau \sin\lambda \tan\lambda \, C_x^y + \sin\Omega\tau \tan\lambda \, C_y^y + \cos\Omega\tau \sin\lambda C_z^y \right] d\tau \\
& + \sin\Omega t \int_0^t \left[\sin\Omega\tau \sin\lambda \tan\lambda \, C_x^y - \cos\Omega\tau \tan\lambda \, C_y^y + \sin\Omega\tau \sin\lambda C_z^y \right] d\tau \Bigg] \\
+ u_{kz} \Bigg[& \cos\lambda \int_0^t C_x^z \, d\tau - \sin\lambda \int_0^t C_z^z \, d\tau \\
& + \cos\Omega t \int_0^t \left[\cos\Omega\tau \sin\lambda \tan\lambda \, C_x^z + \sin\Omega\tau \tan\lambda \, C_y^z + \cos\Omega\tau \sin\lambda C_z^z \right] d\tau \\
& + \sin\Omega t \int_0^t \left[\sin\Omega\tau \sin\lambda \tan\lambda \, C_x^z - \cos\Omega\tau \tan\lambda \, C_y^z + \sin\Omega\tau \sin\lambda C_z^z \right] d\tau \Bigg]
\end{aligned}
$$

$$
\begin{aligned}
\gamma(t) = \; & u_{ky}\Bigg[\cos\Omega t\int_0^t\Big[-\cos\Omega\tilde{\tau}\tan\lambda\, C_x^x - \sin\Omega\tilde{\tau}\sec\lambda\, C_y^x - \cos\Omega\tilde{\tau}\, C_z^x\Big]\,d\tilde{\tau} \\
& \quad + \sin\Omega t\int_0^t\Big[-\sin\Omega\tilde{\tau}\tan\lambda\, C_x^x + \cos\Omega\tilde{\tau}\sec\lambda\, C_y^x - \sin\Omega\tilde{\tau}\, C_z^x\Big]\,d\tilde{\tau}\Bigg] \\
& + u_{ky}\Bigg[\cos\Omega t\int_0^t\Big[-\cos\Omega\tilde{\tau}\tan\lambda\, C_x^y - \sin\Omega\tilde{\tau}\sec\lambda\, C_y^y - \cos\Omega\tilde{\tau}\, C_z^y\Big]\,d\tilde{\tau} \\
& \quad + \sin\Omega t\int_0^t\Big[-\sin\Omega\tilde{\tau}\tan\lambda\, C_x^y + \cos\Omega\tilde{\tau}\sec\lambda\, C_y^y - \sin\Omega\tilde{\tau}\, C_z^y\Big]\,d\tilde{\tau}\Bigg] \\
& + u_{kz}\Bigg[\cos\Omega t\int_0^t\Big[-\cos\Omega\tilde{\tau}\tan\lambda\, C_x^z - \sin\Omega\tilde{\tau}\sec\lambda\, C_y^z - \cos\Omega\tilde{\tau}\, C_z^z\Big]\,d\tilde{\tau} \\
& \quad + \sin\Omega t\int_0^t\Big[-\sin\Omega\tilde{\tau}\tan\lambda\, C_x^z + \cos\Omega\tilde{\tau}\sec\lambda\, C_y^z - \sin\Omega\tilde{\tau}\, C_z^z\Big]\,d\tilde{\tau}\Bigg]
\end{aligned}
$$

APPENDIX C

DERIVATION OF THE MOTION MODEL'S SPECTRA

The model being used to describe the roll angles of a submarine at sea consists of a train of periodic rectangular pulses. The amplitudes of the pulses are normally, or Gaussian, distributed with mean M and standard deviation σ. The sign of the pulses reverses every half period, or T/2, seconds.

The probability density of the amplitudes is

$$p(x) = \frac{1}{\sqrt{2\pi}\,\sigma} e^{\frac{-(x-M)^2}{2\sigma^2}} \qquad \text{(C-1)}$$

The autocorrelation function for this pulse train can be simply determined because of its periodic nature. The autocorrelation function can be constructed by "sliding" an ensemble of pulses along the correlation time (τ) axis, and averaging the product of the displaced and undisplaced ensembles.

For $\tau = 0$, the value of the autocorrelation function is equal to the mean squared value of the pulse train, since no displacement has been made. The mean squared value of a normally distributed quantity is,

$$\phi(0) = \sigma^2 + M^2 \qquad \text{(C-2)}$$

For $\tau = T/2$, negative pulses will fully overlap positive pulses. The autocorrelation function is therefore equal to minus the square of the average of the train, since the pulse amplitudes are independent of their previous values. Thus,

$$\phi(T/2) = -M^2 \qquad \text{(C-3)}$$

For $\tau = T$, positive pulses once more overlap positive pulses, and

$$\phi(T) = M^2 \tag{C-4}$$

It is clear that the autocorrelation function will be periodic hereafter, oscillating between $+M^2$ and $-M^2$. Because the pulses are rectangular, the autocorrelation function will be linear between $+M^2$ and $-M^2$. The autocorrelation function, being an even function, can be plotted as

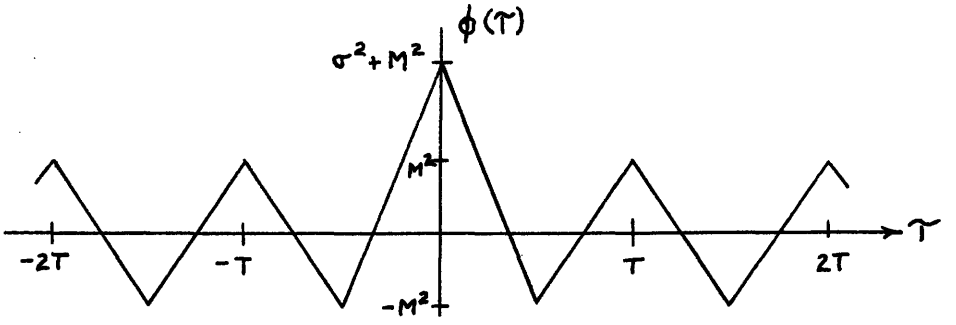

The autocorrelation function can be separated into a periodic component,

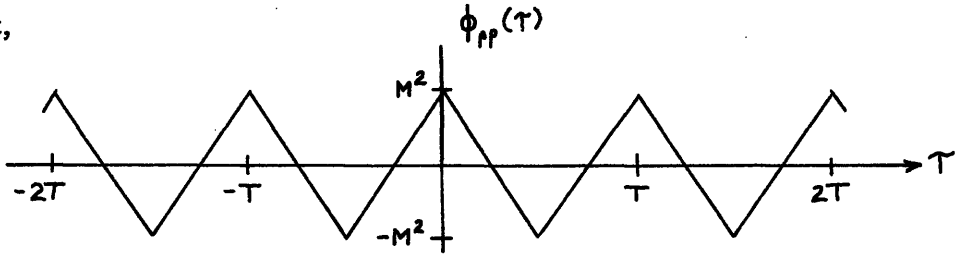

and a random component,

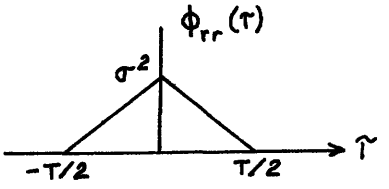

The power spectrum of a periodic autocorrelation function is

$$\Phi_{pp}(n\omega_o) = \frac{2}{T}\int_0^{T/2} \phi_{pp}(\tau)\cos n\omega_o\tau \, d\tau \tag{C-5}$$

where $\omega_o = \frac{2\pi}{T}$. Since

$$\phi_{pp}(\tau) = M^2\left(1-\frac{4\tau}{T}\right) \qquad 0 \le \tau \le T/2 \tag{C-6}$$

the power spectrum is,

$$\Phi_{pp}(n\omega_0) = \frac{2M^2}{T}\int_0^{T/2}\left(1-\frac{4\tau}{T}\right)d\tau$$

$$= M^2\left[\left(\frac{\sin\frac{n\pi}{2}}{\frac{n\pi}{2}}\right)^2 - \frac{\sin n\pi}{n\pi}\right] \qquad n = 0,\pm1,\pm2,\ldots \tag{C-7}$$

For n = 0,±2,±4,...

$$\Phi_{pp}(n\omega_0) = 0 \tag{C-8}$$

and for $n \neq 0$

$$\frac{\sin n\pi}{n\pi} = 0 \tag{C-9}$$

Therefore (C-7) becomes

$$\Phi_{pp}(n\omega_0) = M^2\left(\frac{\sin\frac{n\pi}{2}}{\frac{n\pi}{2}}\right)^2 \qquad n = \pm1,\pm3,\pm5,\ldots \tag{C-10}$$

This power spectrum is plotted below.

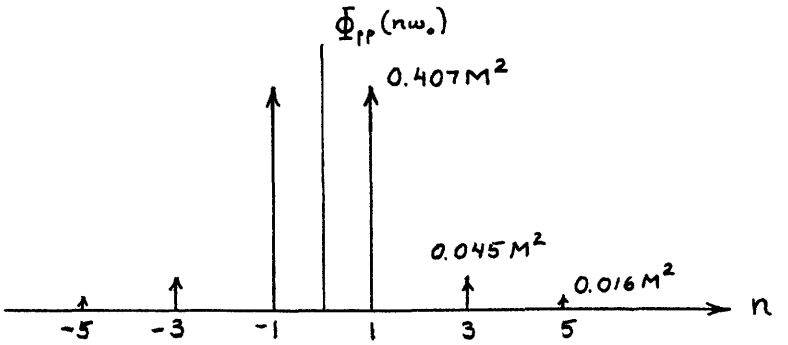

The power density spectrum of a random function is given by

$$\Phi_{rr}(\omega) = \frac{1}{2\pi}\int_{-\infty}^{\infty}\phi_{rr}(\tau)\cos\omega\tau\,d\tau \tag{C-11}$$

The present autocorrelation function is,

$$\phi_{rr}(\tau) = \sigma^2 \left(1 - \frac{2}{T}|\tau|\right) \qquad -T/2 \le \tau \le T/2 \tag{C-12}$$

$$= 0 \qquad \text{elsewhere}$$

Since $\phi_{rr}(\tau)$ is even,

$$\Phi_{rr}(\omega) = \frac{\sigma^2}{\pi} \int_0^{T/2} \left(1 - \frac{2\tau}{T}\right) \cos\omega\tau \, d\tau$$

$$= \frac{\sigma^2}{2\omega_o} \left(\frac{\sin \frac{\omega T}{4}}{\frac{\omega T}{4}}\right)^2 \tag{C-13}$$

This function has been plotted below.

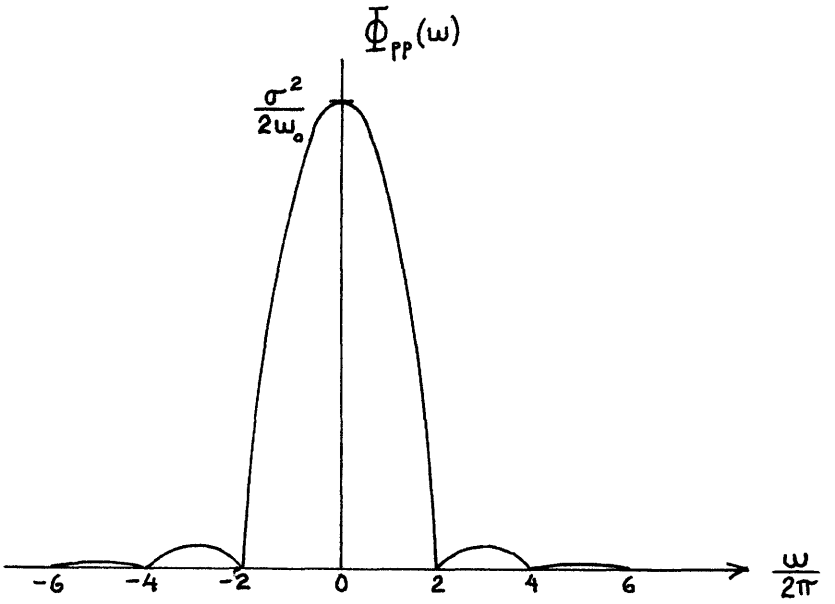

APPENDIX D

BLOCK DIAGRAM OF THE SIMULATION PROGRAM

The digital computer simulations were performed on the Honeywell 800 computer. Programming was done using the MAC language. The running time on the H-800 was approximately 4 minutes for the simulation of a 28 hour operation period.

A block diagram of the simulation program is shown below.

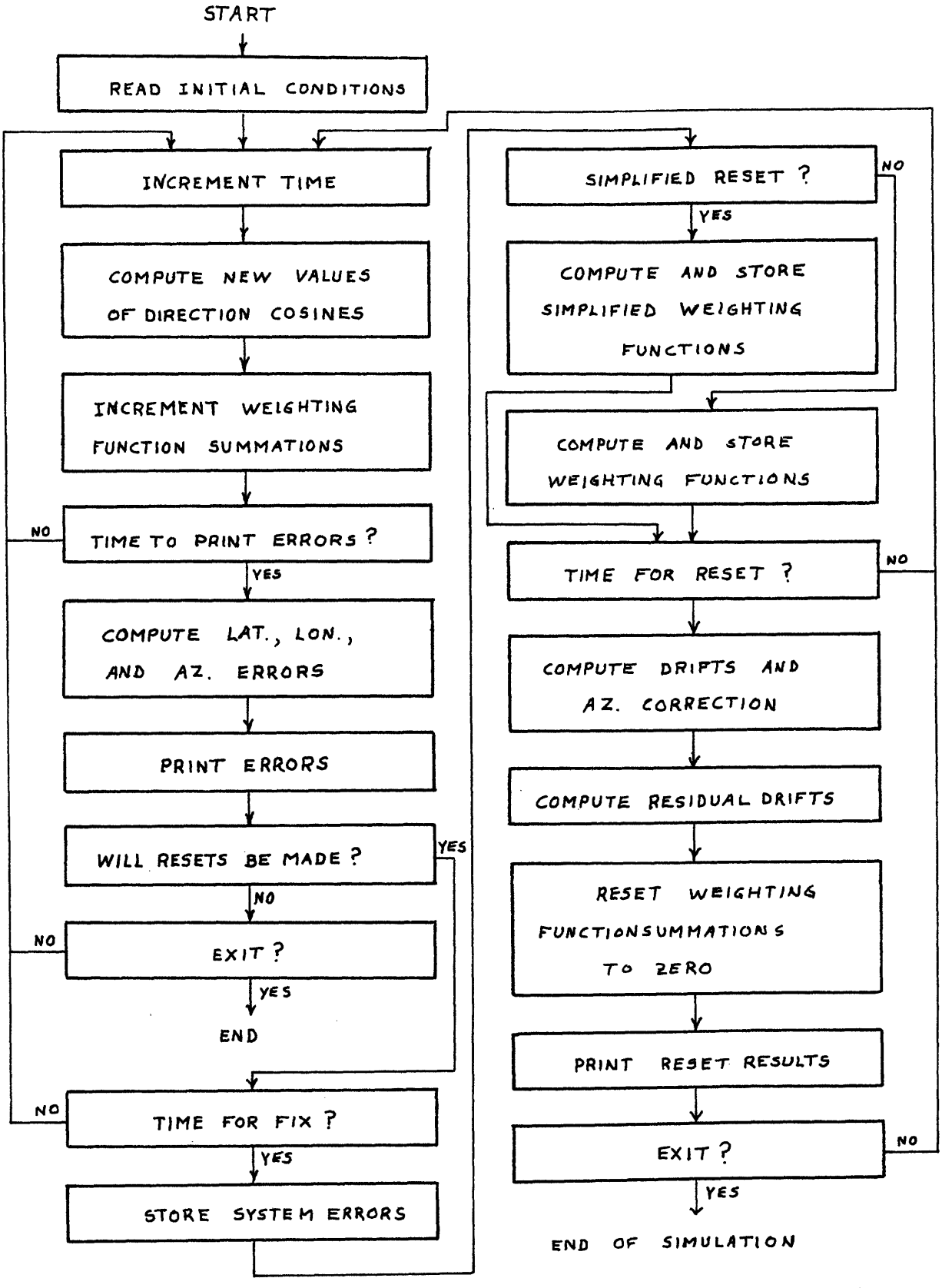
START
READ INITIAL CONDITIONS
INCREMENT TIME
COMPUTE NEW VALUES OF DIRECTION COSINES
INCREMENT WEIGHTING FUNCTION SUMMATIONS
TIME TO PRINT ERRORS ?
NO
YES
COMPUTE LAT., LON., AND AZ. ERRORS
PRINT ERRORS
WILL RESETS BE MADE ?
YES
NO
EXIT ?
NO
YES
END
TIME FOR FIX ?
NO
YES
STORE SYSTEM ERRORS
SIMPLIFIED RESET ?
NO
YES
COMPUTE AND STORE SIMPLIFIED WEIGHTING FUNCTIONS
COMPUTE AND STORE WEIGHTING FUNCTIONS
TIME FOR RESET ?
NO
COMPUTE DRIFTS AND AZ. CORRECTION
COMPUTE RESIDUAL DRIFTS
RESET WEIGHTING FUNCTIONSUMMATIONS TO ZERO
PRINT RESET RESULTS
EXIT ?
NO
YES
END OF SIMULATION

BIBLIOGRAPHY

4. "Theoretical Analysis of Gimballess Inertial Reference Equipment Using Delta-Modulated Instruments," by T. F. Wiener, MIT Doctor of Science Thesis, Report T-300, MIT Instrumentation Laboratory, Massachusetts Institute of Technology, Cambridge, Mass., March, 1962.

5. "The Feasibility of a Gimbal-less Inertial Space Reference," by A. L. Kosmala, Report R-274, MIT Instrumentation Laboratory, Massachusetts Institute of Technology, Cambridge, Mass., April, 1960.

7. "An Investigation of the Computational Errors in a Strapped-Down Inertial System," by E. G. Roby and W. R. Roehrs, MIT Master of Science Thesis, Dept. of Aero. & Astro., Massachusetts Institute of Technology, Cambrige, Mass., June, 1962.

13. "Analysis of an Inertial Navigation System," by Charles Broxmeyer, R-241, MIT Instrumentation Laboratory, Massachusetts Institute of Technology, Cambridge, Mass., August, 1959.

14. "Classical Mechanics," by H. Goldstein, Addison-Wesley, Cambridge, 1950.

15. "Notes on the Single-Degree-of-Freedom Floated, Integrating Gyro," by P. J. Palmer, GL-250, MIT Instrumentation Laboratory, Massachusetts Institute of Technology, Cambridge, Mass., 30 July, 1959.

16. "Dynamic Unbalance in the Single-Degree-of-Freedom Integrating Gyro," GL-204, MIT Instrumentation Laboratory, Massachusetts Institute of Technology, Cambridge, Mass., 20 December, 1954.

17. "Gyro Test Laboratory Unbalance Equations," GT-130, MIT Instrumentation Laboratory, Massachusetts Institute of Technology, Cambridge, Mass., August, 1957.

18. "Gyroscope Unbalance Torques Resulting From Static Linear Compliances," by J. Rossbach, E-508, MIT Instrumentation Laboratory, Massachusetts Institute of Technology, Cambridge, Mass., June 1956.

19. "Vibration Effects on Gyroscopes and Accelerometers," by W. E. Fellows, MH Aero Document R-ED 29004-1A, Minneapolis-Honeywell Regulator Company, Inertial Guidance Facility, St. Petersberg, Florida, 31 October, 1958.

20. "Some Effects of Vibration of Gyroscopic Equipment Performance," by J. M. Buchanan, R-369, MIT Instrumentation Laboratory, Massachusetts Institute of Technology, Cambridge, Mass., July, 1962.

21. "Effect of Angular Vibration on the Performance of a Single-Degree-of-Freedom Integrating Gyroscope", By W. B. Haff and M. Meltzer, Master of Science Thesis, Massachusetts Institute of Technology, Cambridge, Mass., May, 1960.

22. "USS Raton (SSR270) - Spectrum Analysis of Motion Data from Sea Trials," Parts I-V, U.S. Navy Department, David Taylor Model Basin, Hydromechanics Laboratory, 1958.

23. "Damping of Inertial Navigation Systems," by John Hovorka, Doctor of Science Thesis, T-274, MIT Instrumentation Laboratory, Massachusetts Institute of Technology, Cambridge, Mass., May, 1961.

24. "Theory of Seakeeping," by B. V. Korvin - Kroukovsky, The Society of Naval Architects and Marine Engineers, New York 6, New York, 1961.

25. "Statistical Theory of Communication," by Y. W. Lee, John Wiley & Sons, Inc., New York, 1960.

26. "The Mathematics of Circuit Analysis," by E. A. Guillemin, John Wiley & Sons, Inc., New York, 1949.

27. "Electronic Circuits, Signals, and Systems," by S. J. Mason and H. J. Zimmerman, John Wiley & Sons, New York, 1960.

28. "Transients in Linear Systems," by M. F. Garden and J. L. Barnes, John Wiley & Sons, Inc, New York, 1942.

29. "Random Processes in Automatic Control," by J. H. Laning, Jr. and R. H. Battin, McGraw-Hill Book Company, Inc., New York, 1956.